

ATTACHMENT 4

GE Report GENE-0000-0041-1656-01, "Test and Analysis Report, Quad Cities New Design Steam Dryer, Dryer #2 Experimental Modal Analysis and Correlation with Finite Element Results," Revision 2, Non-Proprietary, dated July 2005



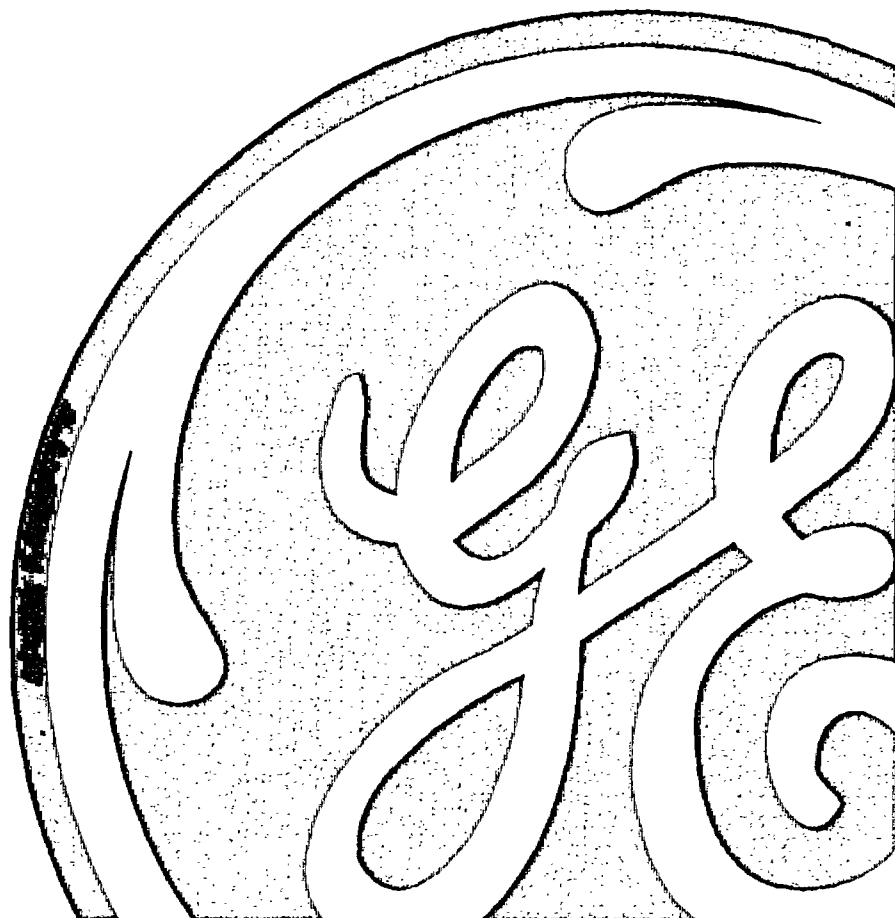
GE Nuclear Energy

General Electric Company
1989 Little Orchard St., San Jose, CA 95125-1030

GENE-0000-0041-1656-01
Revision 2
Class I
DRF-0000-0043-0703
July 2005

NON-PROPRIETARY VERSION

Test and Analysis Report
Quad Cities New Design Steam Dryer
Dryer #2 Experimental Modal Analysis and Correlation with
Finite Element Results, Revision 2



IMPORTANT NOTICE

This is a non-proprietary version of the document GENE-0000-0041-1656-01R2, which has the proprietary information removed. Portions of the document that have been removed are indicated by an open and closed bracket as shown here [[]].

**IMPORTANT NOTICE REGARDING
CONTENTS OF THIS REPORT**

Please Read Carefully

The only undertakings of the General Electric Company (GE) respecting information in this document are contained in the contract between the company receiving this document and GE. Nothing contained in this document shall be construed as changing the applicable contract. The use of this information by anyone other than a customer authorized by GE to have this document, or for any purpose other than that for which it is intended, is not authorized. With respect to any unauthorized use, GE makes no representation or warranty, and assumes no liability as to the completeness, accuracy or usefulness of the information contained in this document, or that its use may not infringe privately owned rights.

Table of Contents

List of Tables	2
List of Figures	2
Acronyms	7
1.0 Executive Summary	8
2.0 Scope	10
3.0 Background	10
4.0 Purpose	11
5.0 Experimental Setup	13
5.1 Test Configuration	13
5.2 Data Acquisition System and Instrumentation	14
5.3 Sensor Locations	15
5.4 Frequency Response Function Measurement Settings	15
5.5 Test Documentation	16
6.0 Test Results	17
6.1 Skirt Damping Measurement Results	17
6.2 Hood Damping Measurement Results	21
6.4 Discussion of Damping Results	23
6.5 Dryer Top Experimental Results	25
6.6 0° Vertical Side Experimental Results	26
6.7 Tie Bar Experimental Results	27
7.0 Correlation	29
7.1 Procedure	29
7.2 Geometric Correlation	29
7.3 Modal Correlation	30
7.4 FRF Correlation	32
7.5 Changes to As-received model	34
8.0 Correlation of Test Results and FE Results	35
8.1 Global Comparison	35
8.2 Skirt Component Comparison	36
8.3 90° Hood Component Comparison	40
8.4 270° Hood Component Comparison	42
9.0 Summary and Conclusions	44
10.0 References	47
Attachment A: Test Plan	96
Attachment B: Hammer Tip Study	110
Attachment C: Effect of Number of Averages	114
Attachment D: Acquisition Front-end channel assignment	121
Attachment E: Test Log Sheets	128

List of Tables

Table 1a: Dryer #2 90° Skirt Damping Results at Low Water Level	18
Table 1b: Dryer #2 270° Skirt Damping Results at Low Water Level	19
Table 1c: Dryer #2 Skirt Damping Results at Low Water Level, Whole Component	20
Table 2a: Dryer #2 Hood Damping Results at Low Water Level	22
Table 2b: Dryer #2 Hood Damping Results at Low Water Level	23
Table 3: Dryer #2 Top Experimental Frequencies	25
Table 4: Dryer #2 0° Vertical Side Experimental Frequencies	26
Table 5: Dryer #2 Tie Bar Experimental Frequencies	28
Table 8: Dryer #2 270° Hood Experimental Frequencies	44

List of Figures

Figure 1: Finite Element Model Representation of Dryer	49
Figure 2: Photograph of Dryer #2, 0° Side	49
Figure 3: Photograph of Dryer #2, 180° Side	50
Figure 4: Tripod Support Attached to Dryer	50
Figure 5: Tripod Support Connection to Dryer	51
Figure 6: Full view of 90 degree hood of Dryer #2 during measurements	51
Figure 7: Pattern of measurement points for the 90 degree hood of Dryer #2, where light red mesh shows the 90 degree hood response locations, dark red represents the responses on top and aqua represents the responses on the ring	52
Figure 8: Response locations on upper right corner of 90 degree hood of Dryer #2	52
Figure 9: Response locations on lower right corner of 90 degree hood of Dryer #2	53
Figure 10: Response location on side panel to the right of main panel of 90 degree hood of Dryer #2 (at angle with respect to main panel)	54
Figure 11: Response locations on upper left corner of 90 degree hood of Dryer #2	55
Figure 12: Response locations on lower left corner of 90 degree hood of Dryer #2 with green circle indicating one of input locations on 90 degree hood	55
Figure 13: Response locations on side panel to the right of main panel of 90 degree hood of Dryer #2 (at angle with respect to main panel)	56
Figure 14: Full view of 270 degree hood of Dryer #2	57
Figure 15: Pattern of measurement points for the 270 degree hood of Dryer #2 where yellow mesh is 270 hood response locations, dark red is responses on top and aqua is responses on the ring	57
Figure 16: Response locations on leftmost panel of 270 degree hood of Dryer #2	58
Figure 17: Response locations on upper part of left middle panel of 270 degree hood of Dryer #2	59
Figure 18: Response locations on upper part of right middle panel of 270 degree hood of Dryer #2	59

GENE-0000-0041-1656-01, Revision 2
Non-proprietary Version

Figure 19: Response locations on lower part of right middle panel of 270 degree hood of Dryer #2..... 60

Figure 20: Response locations on rightmost panel of 270 degree hood of Dryer #2..... 61

Figure 21: Response locations on side panel to the left of main panel of 270 degree hood of Dryer #2 (at angle with respect to main panel)..... 62

Figure 22: Response locations on side panel to the right of main panel of 270 degree hood of Dryer #2 (at angle with respect to main panel)..... 63

Figure 23: Full view of 0 degree side of Dryer #2 (before installation of temporary sensors)..... 64

Figure 24: Pattern of measurement points for the 0 degree side of Dryer #2 where pink mesh is 0 degree side response locations, dark red is responses on top and aqua is responses on the ring..... 64

Figure 25: Response locations on left side of 0 degree side of Dryer #2 with green circle indicating one of input locations on 0 degree side..... 65

Figure 26: Response locations on middle section of 0 degree side of Dryer #2..... 65

Figure 27: Response locations on right part of 0 degree side of Dryer #2..... 66

Figure 28: Full view of 180 degree side of Dryer #2 (before installation of temporary sensors)..... 66

Figure 29: Pattern of measurement points for the 180 degree side of Dryer #2 where blue mesh is 180 hood response locations, dark red is responses on top and aqua is responses on the ring..... 67

Figure 30: Response locations on left part of 180 degree side of Dryer #2..... 67

Figure 31: Response locations on center section of 180 degree side of Dryer #2..... 68

Figure 32: Response locations on right section of 180 degree side of Dryer #2..... 68

Figure 33: Pattern of measurement points for the top, tie bar and inner banks of Dryer #2 where maroon line is 0° side response locations, red is responses on top, pink is tie bar, green is inner bank/perforated panel responses and aqua is responses on the ring..... 69

Figure 34: Response locations on top of Dryer #2, 0° to 90° quadrant..... 70

Figure 35: Response locations on top of Dryer #2, 90° to 180° quadrant..... 70

Figure 36: Response locations on top of Dryer #2, 180° to 270° quadrant..... 71

Figure 37: Response locations on top of Dryer #2, 270° to 0° region..... 71

Figure 38: Close-up of Pattern of measurement points the top, tie bar and inner banks of Dryer #2 where blue mesh is 180 hood response locations, dark red is responses on top and aqua is responses on the ring..... 72

Figure 39: Response locations on tie bar of Dryer #2..... 72

Figure 40: Strain Gage location on tie bar of Dryer #2 – Center gage of rosette was used..... 73

Figure 41: Response locations on tie bar of Dryer #2..... 73

Figure 42: Pattern of measurement points for the skirt and ring of Dryer #2 where purple mesh is skirt response locations, and aqua mesh is the response locations on the ring..... 74

Figure 43: Response locations skirt, 90° panel..... 74

Figure 44: Response locations skirt, 270° panel..... 75

Figure 72: Mode Shapes for Skirt, Local View: Left – [[]].....	90
Figure 73: FE Mode Shape for Skirt [[]].....	90
Figure 74: Mode Shapes for Skirt, Local View: Left – [[]].....	91
Figure 75: Summation FRF for 90°Hood: Red – FE, Green – Test Dryer #1, Blue – Test Dryer #2.....	91
Figure 76: Mode Shapes for 90° Hood, Local View: Left – [[]].....	92
Figure 77: Mode Shapes for 90° Hood, Local View: Left – [[]].....	92
Figure 78: MAC Matrix for 90° Hood, [[]].....	93
Figure 79: Mode Shapes for 90° Hood, Local View: Left – Test, [[]].....	93
Figure 80: Summation FRF for 270° Hood: Red – FE, Green – Test Dryer #1, Blue – Test Dryer #2.....	94
Figure 81: Mode Shapes for 270° Hood, Local View: Top – [[]] Bottom – [[]].....	94
Figure 82: MAC Matrix for 270° Hood, [[]].....	95
Figure 83: Mode Shapes for 270° Hood, Local View: Right – [[]] Left – [[]].....	95
Figure B-1: Comparison of Measurements using Hammer Tips of different hardness, Radial Skirt Response to Radial Skirt Impact (Red curve is soft tip, Green curve is medium tip).....	112
Figure B-2: Comparison of Measurements using Hammer Tips of different hardness, Vertical Side Response to Skirt Impact (Red curve is soft tip, Green curve is medium tip).....	112
Figure B-3: Comparison of Measurements using Hammer Tips of different hardness, 90° Hood Response to Skirt Impact (Red curve is soft tip, Green curve is medium tip).....	113
Figure C-1: Comparison of the FRF amplitude, FRF phase and coherence between a hammer impact measurement with 20 averages (red) and one with 5 averages (green) for normal excitation in point skir:785 and normal response in point skir:785 on the 90 degree skirt panel of dryer 2.....	115
Figure C-2: Comparison of the FRF amplitude, FRF phase and coherence between a hammer impact measurement with 20 averages (red) and one with 5 averages (green) for normal excitation in point skir:785 and normal response in point skir:753 on the 90 degree skirt panel of dryer 2.....	116
Figure C-3: Comparison of the FRF amplitude, FRF phase and coherence between a hammer impact measurement with 20 averages (red) and one with 5 averages (green) for normal excitation in point skir:785 and vertical response in point skir:753 on the 90 degree skirt panel of dryer 2.....	116
Figure C-4: Comparison of the FRF amplitude, FRF phase and coherence between a hammer impact measurement with 20 averages (red) and one with 5 averages (green)	

for normal excitation in point skir:785 and lateral response in point skir:753 on the 90 degree skirt panel of dryer 2..... 117

Figure C-5: Comparison of the FRF amplitude, FRF phase and coherence between a hammer impact measurement with 20 averages (red) and one with 5 averages (green) for normal excitation in point skir:785 and normal response in point skir:707 on the 90 degree skirt panel of dryer 2..... 117

Figure C-6: Comparison of the FRF amplitude, FRF phase and coherence between a hammer impact measurement with 20 averages (red) and one with 5 averages (green) for normal excitation in point skir:785 and vertical response in point skir:707 on the 90 degree skirt panel of dryer 2..... 118

Figure C-7: Comparison of the FRF amplitude, FRF phase and coherence between a hammer impact measurement with 20 averages (red) and one with 5 averages (green) for normal excitation in point skir:785 and lateral response in point skir:707 on the 90 degree skirt panel of dryer 2..... 118

Figure C-8: Comparison of the FRF amplitude, FRF phase and coherence between a hammer impact measurement with 20 averages (red) and one with 5 averages (green) for normal excitation in point skir:785 and normal response in point skir:722 on the 270 degree skirt panel of dryer 2..... 119

Figure C-9: Comparison of the FRF amplitude, FRF phase and coherence between a hammer impact measurement with 20 averages (red) and one with 5 averages (green) for normal excitation in point skir:785 and normal response in point skir:762 on the 270 degree skirt panel of dryer 2..... 119

Figure C-10: Comparison of the FRF amplitude, FRF phase and coherence between a hammer impact measurement with 20 averages (red) and one with 5 averages (green) for normal excitation in point skir:785 and response in strain gage channel C in point skir:796 on the 90 degree skirt panel of dryer 2..... 120

Acronyms

BWR	Boiling Water Reactor
DAS	Data Acquisition System
EMA	Experimental Modal Analysis
EPU	Extended Power Uprate
FE	Finite Element
FEA	Finite Element Analysis
FRF	Frequency Response Function
GE	General Electric
GENE	General Electric Nuclear Energy
MAC	Modal Assurance Criterion
MPT	Mode Pair Table
NPT	Node Pair Table
ODS	Operational Deflection Shape
OLTP	Original Licensed Thermal Power
QC1	Quad Cities Unit 1
QC2	Quad Cities Unit 2
RPV	Reactor Pressure Vessel

1.0 Executive Summary

An experimental modal analysis was performed on new design Dryer #2, the dryer intended for Quad Cities Unit #1 (QC1), and the results were compared to finite element analysis results on a frequency basis and on a mode shape basis. The finite element analysis included a modal analysis and, using those modes from the modal analysis, a mode superposition to obtain FRFs that match the input and response points of the test data. The test results were also compared to the test results of Dryer #1. The Dryer #2 test results showed many similarities to the finite element results and to the Dryer #1 test results.

In terms of frequencies, the finite element model frequencies are generally in good agreement with the test frequencies. For example, the first dominant mode of the 270° skirt panel is at [[]] in the finite element analysis and [[]] in the test results, a difference of 5.1%. The 90° skirt panel, the 90° hood and the 270° hood all had frequency differences between experimental and analytical results of less than 10% for their lowest frequency dominant modes [[

]]

In terms of FRF comparisons, the various components examined showed generally good agreement in trends and levels between summation FRFs for test and FE for that specific component. The 90° hood and the 270° hood were similar to the Dryer #1 results. The most different results were for the 90° skirt panel and the 270° skirt panel. The FRFs on these panels showed similar shapes between Dryer #1 and Dryer #2 but differences in frequency. The 90° skirt panel for Dryer #2 had higher frequencies than that of Dryer #1, and the 270° skirt panel had lower frequencies than Dryer #1.

In addition to determining the natural frequencies and mode shapes, the hammer test responses are used to experimentally determine damping values on the skirt and hood at low water level. The purpose of the experimentally determined damping values was to validate the damping values used in the stress prediction analyses. The damping measurement results showed a range of damping values which validate the damping values used for structural response analyses.

Also, by comparing Dry to LWL measurements for the skirt and the drain channel, it appears that the decrease of damping as frequency increases is caused by the decrease in the effect of water as frequency increases.

From the above discussion on the good agreement of most of the frequency comparisons and the reasonable agreement of the 90° skirt panel first panel mode, it is concluded that the impact hammer test results verify that the finite element model used for dryer design calculations is sufficiently dynamically similar to the as-built dryer for engineering purposes. In addition the impact hammer test results also show that the [[
]] value for the skirt used in the stress prediction analyses are realistic, particularly when considering that the higher force levels expected in operation should produce higher damping levels than obtained in this test.

2.0 Scope

This document summarizes the experimental modal analysis and correlation with finite element results performed to compare the finite element model of the new design steam dryer with the actual production Dryer #2. The experimental modal analysis and the finite element analysis were conducted during early May 2005. The following items are included in this document:

1. Description of the testing performed
2. Presentation of experimental data
3. Description of the finite element analysis
4. Comparison of experimental results with finite element results

3.0 Background

This section provides background information intended to help the reader understand the events that precipitated this program.

The original design BWR steam dryers functioned acceptably at Original Licensed Thermal Power (OLTP) for many years. In response to some cracking of original design and modified original design BWR steam dryers when operation shifted to Extended Power Uprate (EPU), GENE has initiated a program to develop a new design of BWR steam dryer with the design intent of being able to survive loads imposed by EPU. As this design was substantially different from the original design, experimental correlation measurements were considered necessary to determine if the finite element analysis used to predict stresses at EPU with its higher loads correlated to actual hardware fabricated according to the new design. Figure 1 is a depiction of the finite element model for the

new dryer design, and Figures 2 and 3 are pictures of the actual unit, Dryer #2, undergoing final assembly.

4.0 Purpose

The testing and analysis described in this document were defined to accomplish the following main objective:

- Determine if the lowest or first dominant frequencies of major components of the new design steam dryer are within 10% of the frequencies predicted by finite element analysis for the dryer configuration at low water level

The specific purpose of the testing, the experimental modal analysis, is as stated in Reference 1, Steam Dryer Hammer Test Specification, GE 26A6380, Revision 1:

- To identify the as-built frequencies and mode shapes of the dryer's key components at ambient conditions.

These as-built frequencies and mode shapes are to be compared with mode shapes, frequencies and FRFs generated from the finite element model of the dryer.

The program has several side objectives as well:

1. To experimentally measure damping values on the skirt and hood at low water level to validate assumptions used in the stress prediction analyses
2. To provide some limited comparisons to Dryer #1
3. To recommend areas for investigation of differences between model and as-built hardware

4. To recommend areas of improvement of the finite element model to more closely match the as-built hardware

The primary focus of this document is Dryer #2, the dryer intended for Quad Cities Unit #1 (QC1). This dryer will be referred to as Dryer #2 throughout this document. The other dryer is the instrumented dryer intended for Quad Cities Unit #2 (QC2) and is referred to throughout this document as Dryer #1. The construction of the 2 dryers is supposed to be identical except for the modifications necessary for the transducers, conduit and wiring on Dryer #1, the instrumented dryer.

5.0 Experimental Setup

This section describes the test configuration and environment, identifies the instrumentation and data acquisition equipment used, and identifies the sensor locations. The setup and testing follows the requirements outlined in Reference 1, Steam Dryer Hammer Test Specification, GE 26A6380, Revision 1. Attachment A contains the test plan used for the test.

5.1 Test Configuration

Dryer #2, the second dryer with the new design, was tested at J.T. Cullen in Fulton, Illinois, a fabrication facility that served as the location for the installation of the final modifications and for final assembly. For the experimental modal test, the steam dryer was supported in a water tank by 4 tripods with extensions that fit into its main support lug sockets. These tripods were welded to metal plates which were bolted to the concrete floor of the fabrication shop. Figure 4 is a picture of one of the support tripods, and Figure 5 is a close-in picture of the support/dryer connection. A circular tank with a liner was used to hold water for the testing with water. The tank's inner diameter replicated the inner diameter of the reactor pressure vessel (RPV) at the plant to attempt to match the hydrostatic loading at the plant. Testing was performed at 2 different water levels:

1. Dry – no water
2. LWL – Low Water Level – water up to 32.5 inches above the bottom of the bottom flange of the dryer.

All testing was performed at ambient conditions at the test site, with the temperature ranging from 60° F to 75° F

5.2 Data Acquisition System and Instrumentation

The following instrumentation was used to perform the experimental modal analysis and the static test:

1. PCB Model 333A65, 356A22, 356B08, 356B18 and 356A15 triaxial accelerometers, and Model 333B30, 333A32, 333B32, 352C43 and 357B11 single-axis accelerometers
2. PCB Model 086D50 Impact Hammer – Based on operating experience from the Dryer #1 experimental modal and review of its results, the medium hammer tip was selected. Attachment B contains some measurements performed on Dryer #1 comparing the softer hammer tip to the medium hammer tip.
3. PCB Model 086C20 Impact Hammer – This impact hammer was used for the additional drain channel and skirt panel measurements where an impact was performed on a skirt panel or drain channel above the tank upper edge, and a response was measured underwater on the specific skirt panel or on a drain channel. The medium tip was used.
4. Vishay Micro-Measurements CEA-06-125UR-350 Strain Gages
5. Omega LC304-5K Load Cell

The following equipment formed the Data Acquisition System (DAS) and was used to record and analyze the test data:

1. A 116 channel LMS SCADAS III dynamic signal analyzer (2 SCADAS III Model 316 front ends in a Master-Slave configuration) with PQA and PQFA modules was used to provide ICP power to and receive the signal from all of the ICP sensors. For the strain gage measurements, PQBA modules were used in the SCADAS 316 to provide bridge completion and signal conditioning. The system was controlled by a personal computer using LMS Test.Lab 5A software, specifically the Modal Impact, Modal Analysis and Spectral Acquisition modules of software.

5.3 Sensor Locations

The following items detail the contents of Figures 6 through 45 which are pictures that identify the input and response locations used for the experimental modal analysis and that show the test wireframe.

- Figures 6 through 13 show the 90° hood
- Figures 14 through 22 are the 270° hood
- The 0° vertical side locations are shown in Figures 23 through 27
- The 180° vertical side locations are shown in Figures 28 through 32
- Figures 33 through 37 contain the locations on the dryer top
- The tie bar is shown in Figures 38 through 41
- The skirt is shown in Figures 42, 43 and 44
- Figure 45 is an image of the complete test wireframe

5.4 Frequency Response Function Measurement Settings

The signal processing parameters used for data acquisition were the following:

- 5 to 10 averages (1 average for the time domain measurements)
(Attachment C is a comparison of results from 5 averages and 20 averages for one measurement location on Dryer #2 to show that using 5 to 10 averages is adequate. Also, the GE Hammer Test Specification, Reference 2, specifies 3 or more averages)

GENE-0000-0041-1656-01, Revision 2
Non-proprietary Version

- Force window of 20% on the input (Uniform window used for time domain measurements)
- Exponential window of 3% on the responses (Uniform window used for time domain measurements)
- Effective Frequency bandwidth of 400 Hz (actual bandwidth setting 512 Hz, sampling frequency of 1024 Hz) (skirt panel/drain channel had effective frequency bandwidth of 800 Hz, as did time domain measurements – actual bandwidth setting of 1024 Hz, sampling frequency of 2048 Hz)
- 4096 Spectral lines (0.125 Hz resolution/8.0 second time length) (8192 spectral lines for bandwidth settings of 1024 Hz)
- 0.1 second pretrigger on the hammer input

For the measurements, the following results were saved:

- Frequency Response Function
- Coherence
- Input Autopower
- Response Autopowers
- Time Record (for time domain measurements only)

5.5 Test Documentation

Attachment D contains the channel assignment data sheets as referred to in the GE Hammer Test Specification. Attachment E contains the test log sheets.

6.0 Test Results

This section presents a subset of the test results. It covers the damping results based on experimental measurements and other experimental results on components that are not compared to FE results on a component basis. Additional test results that are correlated to FE results are presented in **Section 8.0, Correlation of Test Results and Finite Element Results**.

6.1 Skirt Damping Measurement Results

Measurements were performed to measure the damping on the 90° skirt panel and on the 270° skirt panel at low water level. Acceleration and strain responses were acquired on these panels in response to impacts. Figures 43 and 44 show the impact and response locations for the 90° skirt panel and on the 270° skirt panel, respectively, for the damping measurements.

Damping was calculated in the frequency domain using modal curve-fitting methods on individual FRF measurements and on all of the FRF measurements for the specific component. Reference 2 provides a discussion of the modal curve-fitting method used for the individual FRFs and for the whole component analysis.

The damping results on the skirt are presented in Tables 1a and 1b. Table 1a contains results for individual FRFs on the 90° skirt panel and on the 270° skirt panel while Table 1b contains levels for the whole skirt component.

Table 1a: Dryer #2 90° Skirt Damping Results at Low Water Level

||

||

Table 1b: Dryer #2 270° Skirt Damping Results at Low Water Level

||

||

Table 1c: Dryer #2 Skirt Damping Results at Low Water Level, Whole Component

||

,

,

{3}

The damping in terms of percent critical damping for the individual FRFs ranged from [[]] on the 90° skirt panel, with the higher frequencies generally showing less damping. The 270° skirt panel showed a similar trend, with a range of [[]] In general, the strain gages showed similar to slightly higher damping levels for the same mode than the accelerometers. The overall component damping levels showed a range of [[]] and were generally either similar to or less than the levels derived from individual FRFs.

6.2 Hood Damping Measurement Results

Measurements were performed to measure the damping on the 90° hood and on the 270° hood at low water level. Acceleration was acquired on these panels in response to impacts, and strain was acquired on the 90° hood as well.

Damping was calculated in the frequency domain using modal curve-fitting methods on individual FRF measurements and on all of the FRF measurements for the specific component. Table 2a contains the damping values for the 90° hood, and Table 2b contains the damping values for the 270° hood.

[[

Table 2a: Dryer #2 Hood Damping Results at Low Water Level

]]

[[

Table 2b: Dryer #2 Hood Damping Results at Low Water Level

]]

As with Dryer #1, the hoods of Dryer #2 generally showed less damping than the skirt panels. Percent of critical damping values from the individual FRFs ranged from [[]] on the 90° hood and from [[]] on the 270° hood. Again, damping tended to decrease as frequency increased. On the 90° hood, damping levels derived from individual strain measurements were within the range of the acceleration damping levels or slightly greater than the damping derived from acceleration.

6.4 Discussion of Damping Results

The damping results for Dryer #2 generally match the damping results for Dryer #1. Several questions arise in review of damping results in the previous section. One

question is, “Why does the damping decrease with frequency?” Two possibilities were offered.

1. The input force decreased as frequency increased. Quite often, there is a relationship between input force and measured damping, with damping increasing as input force increases, so possibly in this case the decrease in force versus frequency is also affecting the decrease in damping versus frequency
2. The loading of the water on the lower skirt panel has a greater damping effect at low frequency than high frequency

The 2nd possibility was checked and confirmed by calculating damping for individual FRFs on some of the lower skirt panels and drain channels for both the Dry and LWL conditions. It appears that in the Dry condition, the damping stays relatively constant with frequency while in the LWL condition, damping starts at a significantly higher level at LWL than Dry and decreases to Dry levels. Figures 46 and 47 show the results for lower skirt panel locations and drain channel locations, respectively. These locations are underwater at LWL.

Another question concerned the increase in damping from accelerometer to strain results. Two possibilities are present but no conclusive determination has been made:

1. Some of the strain gages were at the panel edges, greater than 1 inch from the weld but closer than 3 inches, while the accelerometers were in the middle of the panels. It is believed that the edge locations could show more damping than the accelerometer locations. For Dryer #2, some of the strain gages out on the panel among the accelerometers.
2. The strain gage is a displacement-based device while the accelerometer is acceleration-based. There is some belief that this difference is causing a slight increase in damping estimates from strain versus those from acceleration.

Review of damping from strain versus damping from acceleration is still in process as of the writing of this report.

6.5 Dryer Top Experimental Results

This section contains experimental results from the dryer top as well as a limited number of the points on the inner hood and perforated plates. No specific correlation exercise was performed for the dryer top so only the experimental results from curve-fitting up to 150 Hz are presented here.

Table 3: Dryer #2 Top Experimental Frequencies

[[

]]

Table 3 contains significant frequencies for the dryer top below 150 Hz, and Figure 48 contains the summation FRF for the dryer top measurements. The summation FRF is an average of the FRFs in all 3 directions for the included points unless noted. Some of the summation FRFs presented in this report will only be the measurements perpendicular to the surface but will be noted as such.

[[

]]

6.6 0° Vertical Side Experimental Results

As with the dryer top, no specific correlation to finite element results was performed for the 0° vertical side. Figure 41 is the summation FRF for the 0° vertical side, and Table 4 contains significant frequencies for this component below 150 Hz.

Table 4: Dryer #2 0° Vertical Side Experimental Frequencies

[[

]]

Some of the same observations as those made for Dryer #1 are made:

[[

]]

One new observation, but somewhat similar to the last one above, is that the high modal density of the vertical side starts at [[]] many modes of the 0° vertical side were obtained during curve-fitting.

The measurements for the 180° vertical side were included after the poles were selected, and various modes of the 0° vertical side appeared as in-phase or out-of-phase with similar shapes of the 180° vertical side, although often the amplitude of the 180° vertical side is lower because it is assumed that the mode shapes of the sides were at slightly different frequencies, and the 0° vertical side modes were the modes being fit.

6.7 Tie Bar Experimental Results

The experimental results for one section of one of the tie bars, the portion nearest the 90° hood of the tie bar nearest the 180° side, are presented in this section. On the instrumented dryer, this tie bar has strain gage S6 located along it longitudinally, near the middle of the right span in Figure 40 to the right of location 1002 and its accelerometer where the temporary strain gage is located. No correlation to finite element results was performed for the tie bar. Figure 50 is the summation FRF for the tie bar up to 150 Hz, and Figure 51 is the summation FRF of the tie bar up to 500 Hz. Table 5 contains significant frequencies for this component. Curve-fitting on this component was performed up to 500 Hz because the most significant peak appears [[]] and the summation FRF is relatively flat (but sloping higher in amplitude as frequency increases) with many small peaks up to that frequency. It is assumed that [[]] is the first bending mode of that span; however, there are not enough sensor locations on it to definitively make that conclusion. Figure 52 is a plot of the FRF with the response from a strain gage located where permanent sensor S6 is located on Dryer #1 and the input from an impact hammer hitting this span near the strain gage.

Table 5: Dryer #2 Tie Bar Experimental Frequencies

[[

,

,

]]

7.0 Correlation

This section discusses the process of using finite element model results to correlate with experimental test results.

7.1 Procedure

The goal of the correlation is to determine the differences between the FE model and the test object and to determine the sensitive spots of the FE model. Afterwards, one can improve the correlation, focusing on those hot spots, and finally obtain a model that is more realistic than the previous one.

The correlation procedure contains the following steps:

- Geometric correlation: Definition of a relationship between the units, the coordinate systems and the measuring points of the TEST model on one hand, and the units, the coordinate systems and the nodes of the FE model on the other hand.
- Modal correlation: Comparison of the experimental mode shapes and the FE mode shapes, based on wireframe animations and MAC (modal assurance criterion) calculations.
- Correlation of the transfer functions: Comparison of the measured FRFs and the ones calculated directly or synthesized from the FE mode shapes.

The calculations of the FE mode shapes and FRFs have been done here with ANSYS 8.1. The correlation has mainly been done in LMS/LINK and Test.Lab.

7.2 Geometric Correlation

This phase ensures the compatibility between the measured and the calculated data. It includes the following steps:

1. Definition of rational entities/groups in the model, grouping nodes that have common properties or are part of the same panel for example. Those entities are called components.
2. Definition of pairs between TEST measuring points and FE nodes. These pairs are stored in a node pair table (NPT). This table allows the automatic projection of the TEST geometry on the FE geometry.
3. Compatibility between the global and local coordinate systems. This information is also contained in the node pair table and ensures a proper projection of the TEST geometry on the FE geometry.
4. Transformation of the TEST data (modes, FRFs, wireframes) to the verification system (FE model), in order to make the comparison easier.

All these steps were done in LMS/LINK.

7.3 Modal Correlation

The dynamic behavior of a structure, at least in the low frequency range, is best described by its normal modes. From experimental normal analysis, the modes of the structural components are known with their shapes, frequencies, and modal damping.

For the FE model, shapes and frequencies of normal modes are calculated in ANSYS 8.1 (analysis ANTYPE, 2). For the test results, the general process has been to calculate the complex modes first, review those modes, and then use the same poles to calculate the normal modes for direct comparison with FE results.

Experimental modes can be directly compared to FE modes by using the wireframe animations from both Test and FE. Using this technique, important conclusions can be drawn regarding parts that are not well modeled in the FE.

After the first mode extraction for example, four grounded springs were added to the model as boundary condition. These grounded springs (COMBIN14) were fixed to the

dryer ring in the 4 support points. This was intended to model as simply as possible the support beams used in the test rig that support the dryer. This was necessary to be able to extract the suspension modes and model the influence that the supports have on the rest of the structure as there was concern that the support stiffness influenced some of the lower frequency flexible modes of the dryer.

Of course, FE modes can also be visualized with the entire model, and not only the wireframe geometry. This way, one can easily understand the real nature of the modes, which is not always obvious with wireframe animations.

Another tool to judge modal correlation is the Modal Assurance Criterion (MAC). It expresses the nature of the relationship between two sets of vectors. For each pair of modes compared, it is calculated from the vectors of each degree of freedom considered in the correlation model. Mathematically, the MAC is defined as

$$MAC_{rr'} = \frac{|\{\Psi_r^{test}\} \{\Psi_{r'}^{FE}\}|^2}{(\{\Psi_r^{test}\} \{\Psi_r^{test}\}^*) (\{\Psi_{r'}^{FE}\} \{\Psi_{r'}^{FE}\}^*)}$$

where (Ψ_r^{test}) is a modal vector from test and $(\Psi_{r'}^{FE})$ is a modal vector from the finite element solution. These modal vectors each represent a single frequency and contain the common degrees of freedom between the test and the FE, in this case on a component basis. For identical modes, the MAC is 1. For linearly independent mode shapes, the MAC is 0. As the MAC formulation includes a quadratic term, small or local deviations between Test and FE will result in considerably lowered MAC values.

Unfortunately, the FE modal density at low frequency is already very high for the dryer. And too many local effects are already present at the very low frequencies (this is a direct result of the low stiffness of the perforated inner panels of the dryer). As a result, the global modes are mixed/lost among many local modes. For example here, in the 200 first

FE modes, only 10 had global characteristics; all of the other modes were 1st, 2nd and 3rd bending modes of the inner perforated panels.

On the other hand, the low number of measuring points on a region makes it impossible to capture those local modes in the experimental TEST modal analysis.

As result, one TEST mode corresponds to many FE modes, global, local or mixed. A one-to-one TEST-FE mode comparison is thus very difficult, and makes it difficult to draw any conclusion of the MAC analysis.

The MAC analysis was still used, but generally only after visual inspection of the mode shapes and of the summation FRFs had narrowed down the frequency range to be examined.

7.4 FRF Correlation

Normal modes are an efficient representation of the dynamic behavior of a structure, but only useful for correlation as long as the modes are not combining too many local effects. As mentioned above, even at low frequency, there are many local modes. This quantity of local modes means that the local effects of one FE mode usually occur at multiple frequencies in the test model. As a consequence, one FE mode will partially correlate with multiple test modes. Also, a test mode will combine multiple local effects that correlate partially with multiple FE modes. This makes it very difficult to find the same combination of the same local effects in test and FE. As long as the same local effects occur at approximately the same frequency, a good dynamic correlation is obtained, even if this is not visible in a MAC matrix.

Another way thus to compare dynamic behavior of two models is looking at frequency response functions (FRFs). They can be evaluated over the whole frequency range of interest. In an FRF, the (acceleration) response of one point is plotted as function of a unit

(force) input in another point. Modes can be found as peaks in an FRF, and the higher the modal damping, the lower and broader the peak will be.

For checking correlation, the synthesized FE FRFs are compared with the corresponding measured test FRFs. More interesting than the exact amplitude is the general shape of a FRF. A good correlation means that important peaks from the test should be found in the synthesized FRFs at a similar frequency, and the general amplitude of the FE and test FRFs are similar.

A FRF can be calculated in ANSYS with the harmonic response analysis (ANTYPE, HARMIC). The idea is to impose a unitary force in one DOF of the hitting points and calculate the frequency response (displacements or accelerations) in all the DOFs of all the other points. The obtained response functions can then effectively be seen as displacements or accelerations per unit input force.

Three methods of solution are available in ANSYS to calculate FRFs with the harmonic response analysis:

1. Full (HROPT, FULL)

This method solves the general equation of motion of a structural system transposed in frequency domain directly.

2. Reduced (HROPT, REDUC)

The reduced solution method uses reduced structure matrices to solve the equation of motion. This method runs faster than the full harmonic response by several orders of magnitudes, because the technique of matrix reduction is used so that the matrix used to represent the system is reduced to the essential DOFs required to characterize the response of the system.

3. Mode superposition (HROPT, MSUP)

The mode superposition method uses the natural frequencies and mode shapes from the modal analysis (ANTYPE, MODAL) to compute the dynamic response to steady harmonic excitation. It converts the equation of motion in its modal form. The advantage of this method is that the computationally expensive matrix algebra can be calculated inexpensively in modal coordinates. The individual modal responses are then superimposed to obtain the actual response.

The Full method is very memory and time-consuming and was not used in this project. The Mode Superposition technique was preferred here. This method has as an advantage that the mode shapes only have to be calculated once and can be re-used to calculate FRFs for different input points. On the other hand, the reduced and full harmonic methods have to be repeated for each hitting point. Some FRFs were generated in LMS Link software using mode superposition as well.

7.5 Changes to As-received model

Several changes were made to the model after it was received from GE to more closely replicate the test conditions.

- Elastic modulus and damping changed to ambient conditions from reactor conditions (the lower skirt super element with its loading by water was left unchanged)
- Removal of pressure loading (a pressure loading from reactor conditions)
- Addition of grounded springs instead of perfectly rigid constraints at the support locations (the dryer as tested was supported on stands that exhibited flexibility as compared to the completely rigid FE constraints. A complete iteration of these springs to match the test results was not performed.)

8.0 Correlation of Test Results and FE Results

This section presents comparisons between test results and finite element analysis results on several levels:

- Global
- Skirt Component
- 90° Hood Component
- 270° Hood Component

The comparisons are presented as comparisons of frequencies, comparison of test FRFs to FE FRFs, comparison of local mode shapes and comparison of global mode shapes. Comparison started on a global level and moved to a component level due to the many closely spaced modes of some of the dryer components in the finite element model. Because of the modal density, many of the test modes appear similar to numerous FE modes, making it very difficult to find a single corresponding mode. Correlation on a component basis was performed by observing significant peaks in the summation FRF and some individual FRFs of the component to narrow down the frequency range for searching the FE modes and then reviewing the mode shape animations and MAC matrices for the test and FE components. Also, for the skirt and both hoods, 2 relatively widely spaced peaks in the frequency domain were examined. After that review, the other components were added to the mode shape to observe the global mode that the component mode was related to.

8.1 Global Comparison

The results from the experimental modal and the finite element analyses have not been directly compared on a global level, but similarities have arose as the component comparisons were being performed. There are similar modes under 10 Hz that are

directly controlled by the modeling of the supports and the local region of the dryer that the supports attach to. For this study, it was decided to stop the iterative adjustment of the support springs as its effect on the component modes was expected to be minimal, but this adjustment is still an area for potential improvement.

The first significant global flexible mode is found at [[]] a mode in which the hoods appear to slide laterally out of phase with each other with what appears to be a twist or rotation of the skirt and ring. This specific global test mode for Dryer #2 is [[]] of the same mode for Dryer #1. The finite element counterpart to this mode ended up at [[]] with the grounded springs used at the support locations. Possibly this frequency difference could possibly be reduced further through adjustment of the grounded spring supports or possibly other parameters; however, as mentioned above, it was decided to stop iterating the FE grounded springs to match the test.

8.2 Skirt Component Comparison

The skirt was the first component to be analyzed on a component basis. Table 6 contains frequencies from the test data analysis and a limited number of frequencies from the finite element results. Figure 53 contains the skirt summation FRF, a comparison among test results for both Dryer #1 and Dryer #2 and FE results for the whole skirt. This summation FRF used only the points common between Dryer#2 and Dryer #1. Dryer #2 utilized all of the Dryer #1 points but also included additional points on the 90° skirt panel and on the 270° skirt panel. Figure 54 is a summation FRF for all of the points measured for Dryer #2. A summation FRF for the 90° skirt panel is included as Figure 55. Figures 56 and 57 contain individual FRF comparisons between FE, Dryer #1 and Dryer #2 for the 90° skirt panel. Figure 58 is a comparison between test Dryer #1 and Dryer #2 for a different input point than the preceding figures for the 90° skirt panel. The shapes of the Dryer #1 and Dryer #2 summation FRFs compare well for both the whole component and the skirt panels, but some frequencies have shifted. For the 90° skirt

panel, the Dryer #2 frequencies are consistently higher than those for Dryer #1. Figure 58 illustrates this increase well. The 270° skirt panel will be discussed farther into this section.

Table 6: Dryer #2 Skirt Experimental Frequencies

[[

]]
For the 90° skirt panel, the first panel bending mode appears [[]]] for the test while it is [[]]] for the FE result. Figure 59 is the MAC matrix used to find the similar modes in this frequency range. The FRFs and the animations were then reviewed as well to make the link between test and FE. Figure 60 is a comparison of static depictions from the animations of the test and FE modes while Figure 61 is a

representation of the complete FE model for this mode (as opposed to only the test points).

The second mode of the 90° skirt panels appears to be at approximately 10% from the finite element prediction ([[] for Test, [] for FE). Figure 62 is the MAC matrix for this frequency range, and Figure 63 is the mode shape comparison of these modes. Note that the test mode does appear to be slightly diagonal as opposed to purely vertical. It is believed that this diagonality on Dryer #1, coupled with only measuring 2 points on the skirt panel, led to difficulty distinguishing between the 2nd vertical and 2nd lateral bending modes for the 90° skirt panel. Figure 64 is the finite element mode shape []

Figure 65 is the 2nd lateral bending mode of the 90° skirt panel – at [] for test and [] for FE. Again, the test mode is somewhat diagonal, not purely lateral. The finite element mode shape for [] is contained in Figure 66.

Figure 67 is the summation FRF for the 270° skirt panel. Figures 68 and 69 are comparisons of the test measurements for both Dryer #1 and Dryer #2 on the 270° skirt panel along with FE predictions, and Figure 70 compares FRFs for Dryer #1 and Dryer #2 for a different input point than the previous figures. It appears that the first panel mode of the 270° skirt panel is at [] and it matches best with a [] FE mode, although the phasing with the 90° skirt panel does not match between test and FE results. Figure 61 illustrates the MAC matrix for this frequency range. Figure 71 is a static depiction of the mode shape comparison for the first panel mode of the 270° skirt panel.

In FE the 2nd panel mode of the 270° skirt panel is [] This 2nd panel mode is most clearly similar to a test frequency of [] and the shape comparison is

shown in Figure 72. Figure 62 is the MAC matrix used to help narrow down the comparison.

Figure 73 shows the finite element representation of the [[]] mode shape, a similar mode shape to the [[]] FE mode shape. The 2nd lateral panel mode for the 270° skirt panel appears to match the 90° skirt panel frequency [[]] for test and [[]] for FE. In this mode shape, the 90° skirt panel and the 270° skirt panel are out-of-phase. Also, while difficult to observe in the static depiction, the animation shows that the mode shape for the 270° skirt panel is more purely lateral than the 90° skirt panel.

8.3 90° Hood Component Comparison

The 90° hood test results were compared to finite element predictions and in a limited fashion to Dryer #1. Figure 75 is the summation FRF for this component – a comparison of FE, Test Dryer #1 and Test Dryer #2. As with the other components examined, the [[]] global mode clearly appears. The general trend of the FRFs from Dryer #1 and Dryer #2 are very similar in both shape and frequency. Table 7 contains the test mode frequencies for Dryer #2 and comparisons with several FE mode frequencies.

[[

]]

For the 90° hood upper frequency range around [[]] similar modes emerged in both the visual comparison and the MAC calculation for the frequency range [[]] Figure 77 compares mode shapes at [[]] Figure 78 is a MAC matrix of the frequency range [[]] that shows a cluster of test modes being very similar to a larger cluster of FE modes. The [[]]test mode and [[]]FE mode were chosen by viewing this MAC matrix in conjunction with review of frequency of the peaks of the summation FRFs and the mode shape animations. For Dryer #1, the test mode in this frequency range was [[]]

Another mode was compared for the 90° hood. Figure 79 is a static depiction of a mode shape that appears in the test results [[]] and in the FE results [[]].

Table 7: Dryer #2 90° Hood Experimental Frequencies

[[

]]

8.4 270° Hood Component Comparison

The 270° hood test results were compared to finite element predictions at frequencies similar to the frequency regions used for the 90° hood. Table 8 contains the significant test modes and frequencies of similar FE modes. As with the other components evaluated the global mode [[]] was present. For the 270° hood, the first flexible mode, although one related to significant skirt activity, appears at [[

]] Figure 80 compares Dryer #1 and Dryer #2 test summation FRFs with an FE summation FRFs.

Figure 81 shows a comparison of component-level mode shapes at [[
]] This difference in frequency is [[
]] although there is a cluster of [[
]] is similar to.

As for the 90° hood, the other frequency range of interest for the 270° hood is the [[
]] region. Figure 82 contains the MAC matrix display with the FE results in the 85 Hz to 95 Hz frequency range. Again, the [[

]] It is most similar to a [[
]] FE mode, shown in Figure 83 on a component level. The Dryer #1 test mode was at [[
]]

Table 8: Dryer #2 270° Hood Experimental Frequencies

[[

]]

A general observation of the summation FRFs for the 270° hood is that the level of the FRF predicted by FE is lower in the [[]] region. This difference can be seen in Figure 80. The hood in FE may be too stiff or its connections may be too stiff as the general trend of the FE versus test comparison for the hood is that the FE levels are lower than the test levels.

9.0 Summary and Conclusions

An experimental modal analysis was performed on new design Dryer #2, the dryer intended for Quad Cities Unit #1 (QC1), and the results were compared to finite element analysis results on a frequency basis and on a mode shape basis as well as to results from the experimental modal analysis on Dryer #1. The finite element analysis included a

modal analysis and, using those modes from the modal analysis, a mode superposition to obtain FRFs that match the input and response points of the test data. The test results showed many similarities to the finite element results and to the Dryer #1 test results. In terms of frequencies, the trend is that the finite element model frequencies are generally in good agreement with the test frequencies. For example, the first dominant mode of the 270° skirt panel is [[]] in the finite element analysis and [[]] in the test results, a difference of [[]]. The 90° skirt panel, the 90° hood and the 270° hood all had frequency differences between experimental and analytical results of [[]] for their lowest frequency dominant modes except for the 90° skirt panel first panel mode where the test frequency was [[]] the FE frequency and higher than the similar Dryer #1 frequency as well.

In terms of FRF comparisons, the various components examined showed generally good agreement in trends and levels between summation FRFs for test and FE for that specific component. The most different results were for the 90° skirt panel and the 270° skirt panel which showed similar shapes between Dryer #1 and Dryer #2 but differences in frequency. The 90° skirt panel for Dryer #2 had higher frequencies than that of Dryer #1, and the 270° skirt panel had lower frequencies than Dryer #1.

The decrease in test versus finite element agreement as frequency increases is expected because, as the mode shapes become more complex with higher frequency, the finite element model results become more sensitive to several parameters such as boundary condition details, element type and number of elements. The boundary conditions of the individual plates, the welds to other plates and beams, are not explicitly modeled in the finite element model. The wavelengths of the higher modes are shorter so more elements are needed to accurately represent the shapes; however, increasing the number of elements prohibitively increases computation time. The lower skirt super element, which includes hydrodynamic effects of the water on the skirt up to Low Water Level (LWL),

may have some effect on the higher mode frequencies and test versus finite element differences as well.

In addition to determining the natural frequencies and mode shapes, the hammer test responses are used to experimentally determine damping values on the skirt and hood at low water level. The purpose of the experimentally determined damping values was to validate the damping values used in the stress prediction analyses. The damping measurement results showed a range of damping values which form a technical basis for arriving at appropriate damping values to be used for structural response analyses.

Also, by comparing Dry to LWL measurements for the skirt and the drain channel, it appears that the decrease of damping as frequency increases is caused by the decrease in the effect of water as frequency increases.

From the above discussion on the good agreement of most of the frequency comparisons and the reasonable agreement of the 90° skirt panel first panel mode, it is concluded that the impact hammer test results verify that the finite element model used for dryer design calculations is sufficiently dynamically similar to the as-built dryer for engineering purposes. In addition the impact hammer test results also show that the [[
]] used in the stress prediction analyses are realistic, particularly when considering that the higher force levels expected in operation should produce higher damping levels than obtained in this test.

10.0 References

1. Ramani, Venkat “Steam Dryer Hammer Test Specification.” GE 26A6380. GENE. San Jose, CA. April 2005.
2. Peeters, Bart; Guillame, Patrick; Van der Auweraer, Herman; Cauberghe, Bart; Verboven, Peter; Leuridan, Jan. “Automotive and Aerospace Applications of the PolyMAX Modal Parameter Estimation Method.” Proceedings of International Modal Analysis Conference (IMAC) 22. Dearborn, MI. January, 2004.

Figures

[[

Figure 1: Finite Element Model Representation of Dryer

]]



Figure 2: Photograph of Dryer #2, 0° Side



Figure 3: Photograph of Dryer #2, 180° Side



Figure 4: Tripod Support Attached to Dryer

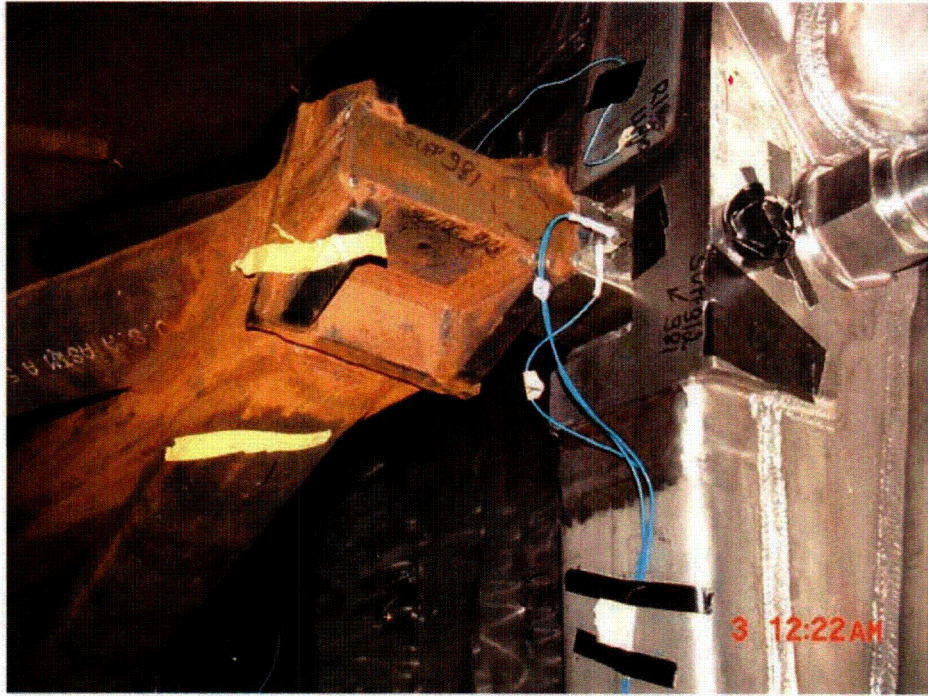


Figure 5: Tripod Support Connection to Dryer

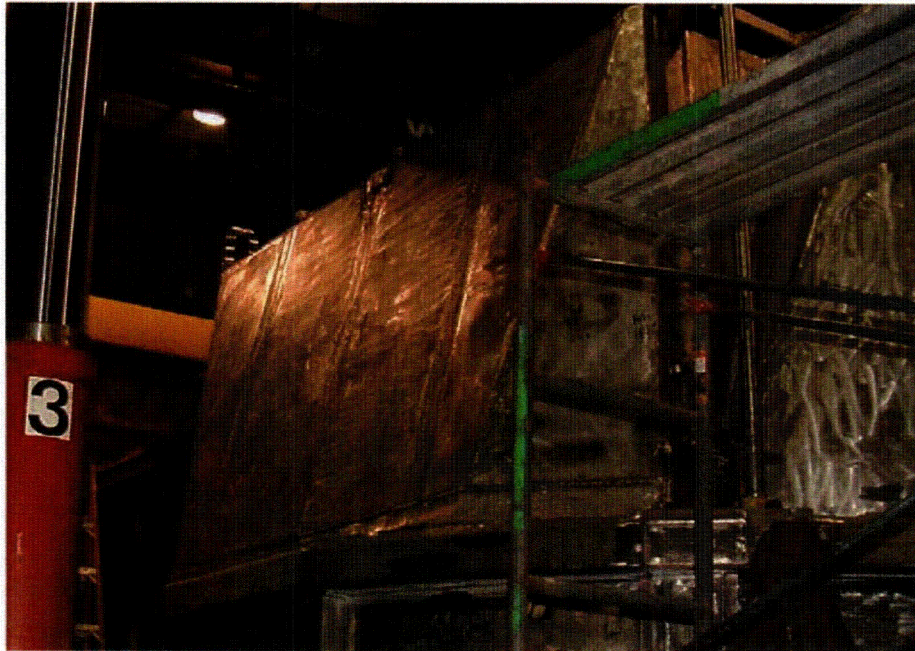


Figure 6: Full view of 90 degree hood of Dryer #2 during measurements.

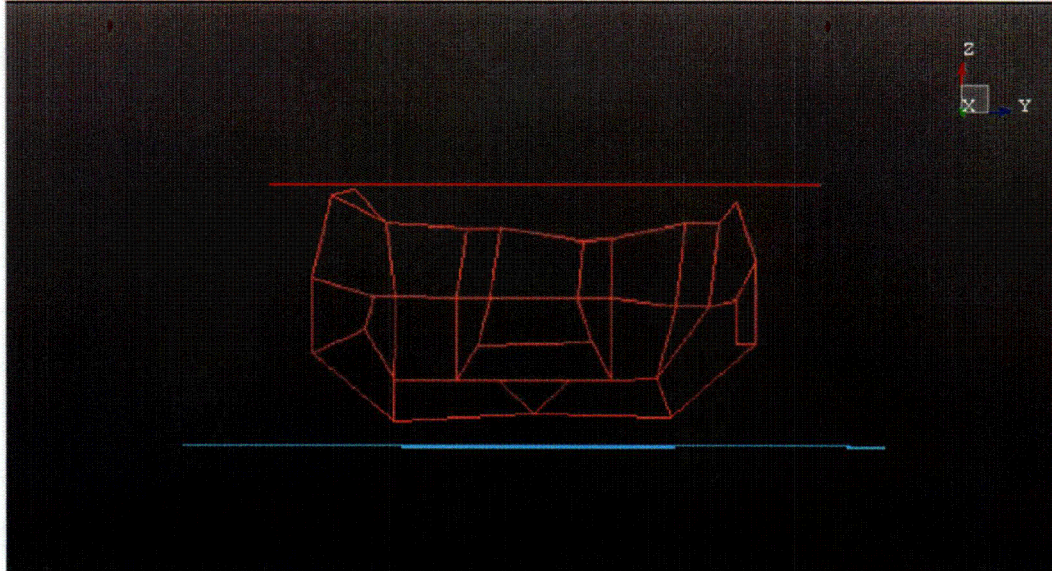


Figure 7: Pattern of measurement points for the 90 degree hood of Dryer #2, where light red mesh shows the 90 degree hood response locations, dark red represents the responses on top and aqua represents the responses on the ring.

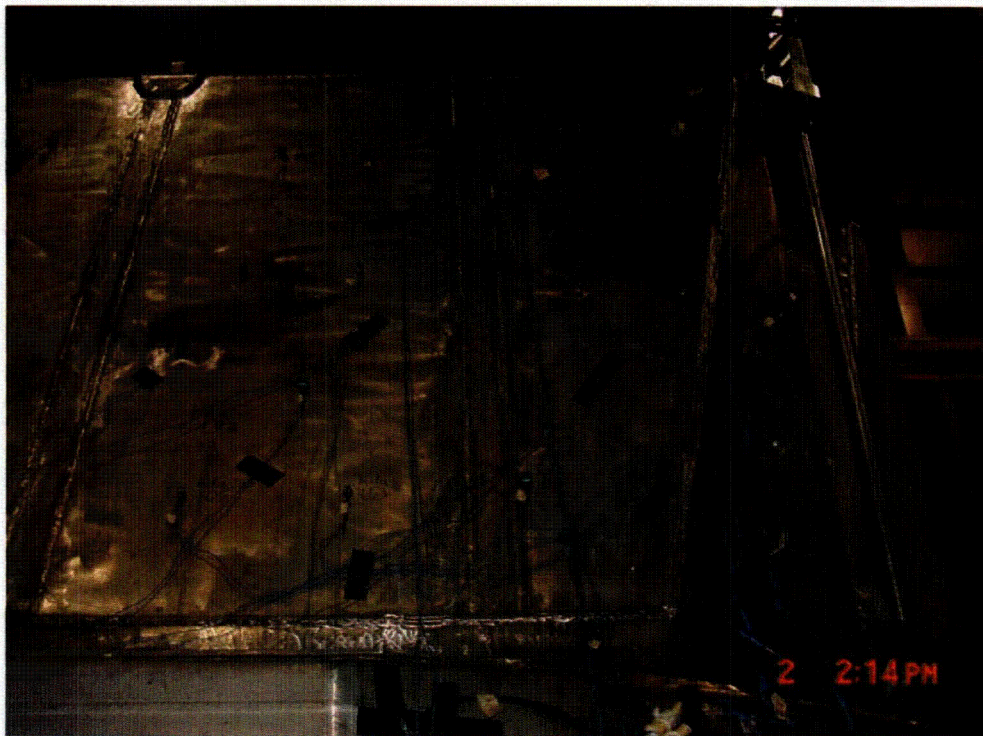


Figure 8: Response locations on upper right corner of 90 degree hood of Dryer #2.

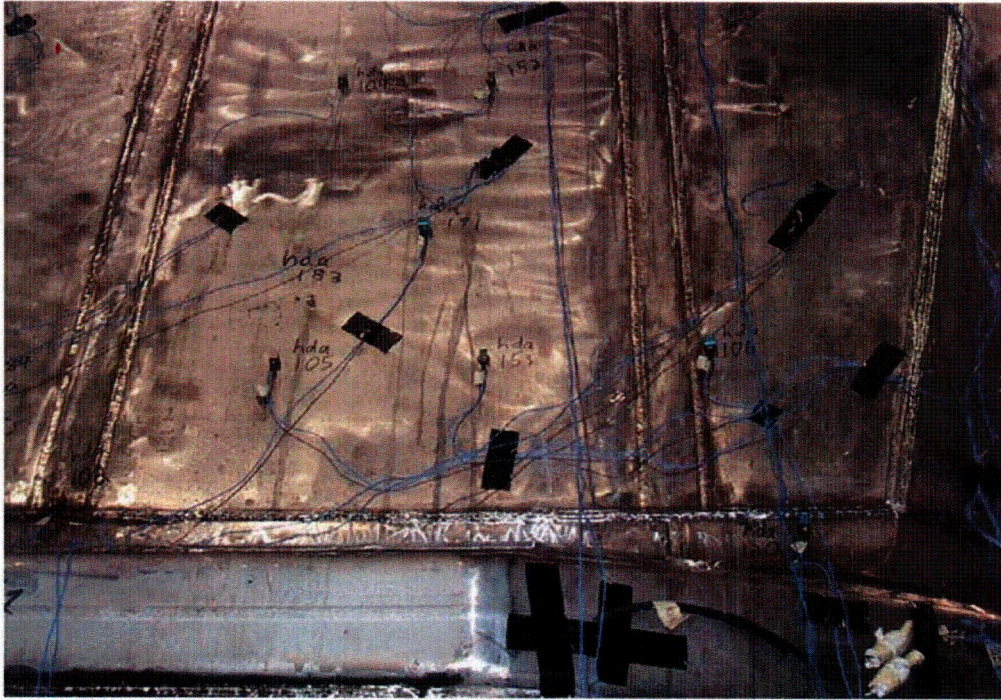


Figure 9: Response locations on lower right corner of 90 degree hood of Dryer #2.

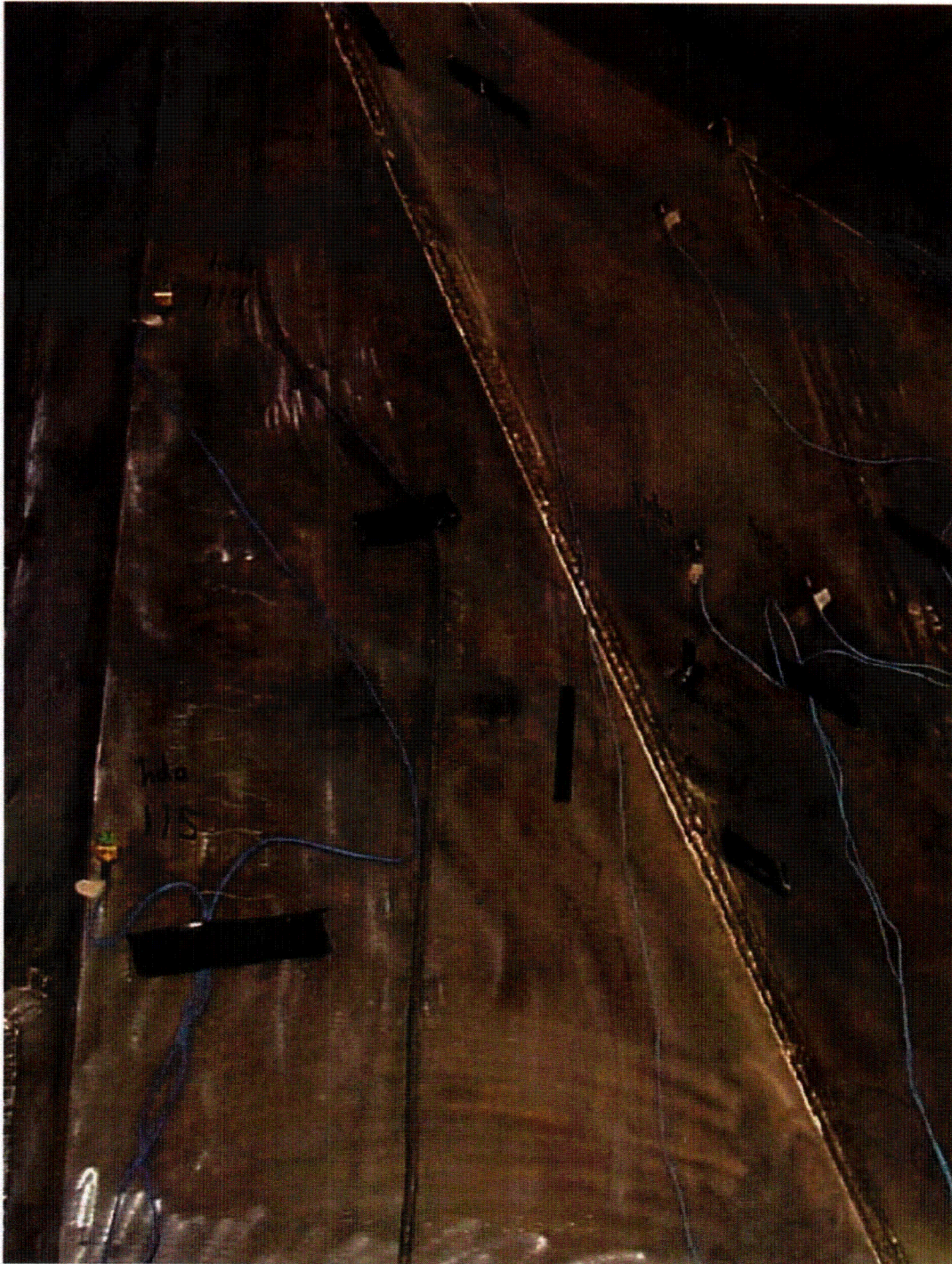


Figure 10: Response location on side panel to the right of main panel of 90 degree hood of Dryer #2 (at angle with respect to. main panel).



Figure 11: Response locations on upper left corner of 90 degree hood of Dryer #2.

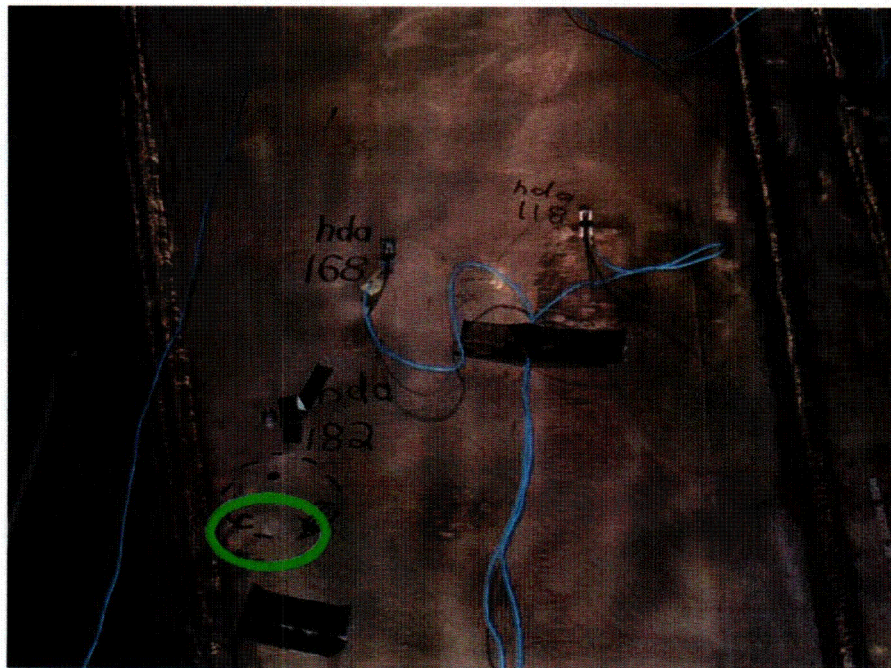


Figure 12: Response locations on lower left corner of 90 degree hood of Dryer #2 with green circle indicating one of input locations on 90 degree hood.



Figure 13: Response locations on side panel to the right of main panel of 90 degree hood of Dryer #2 (at angle with respect to main panel).



Figure 14: Full view of 270 degree hood of Dryer #2.

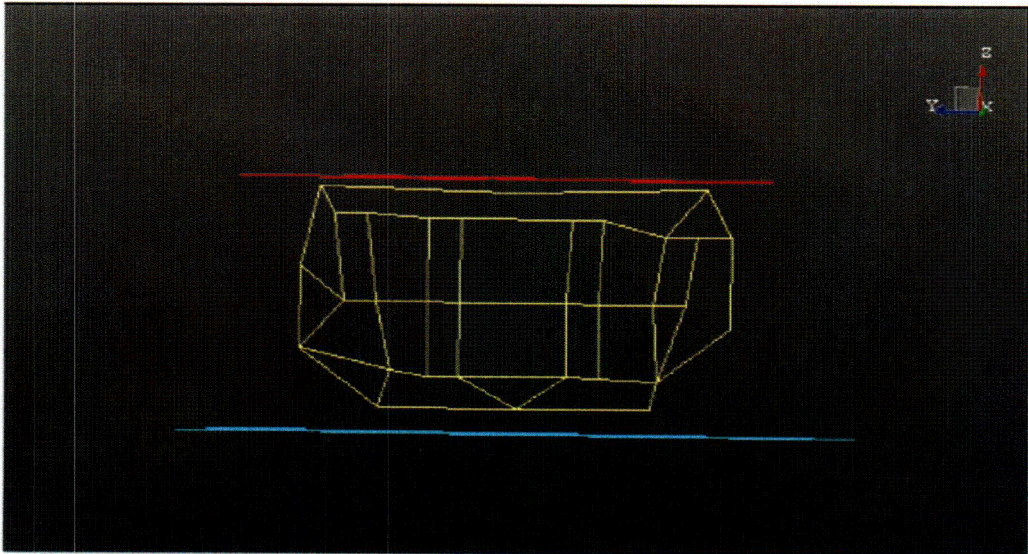


Figure 15: Pattern of measurement points for the 270 degree hood of Dryer #2 where yellow mesh is 270 hood response locations, dark red is responses on top and aqua is responses on the ring.



Figure 16: Response locations on leftmost panel of 270 degree hood of Dryer #2.

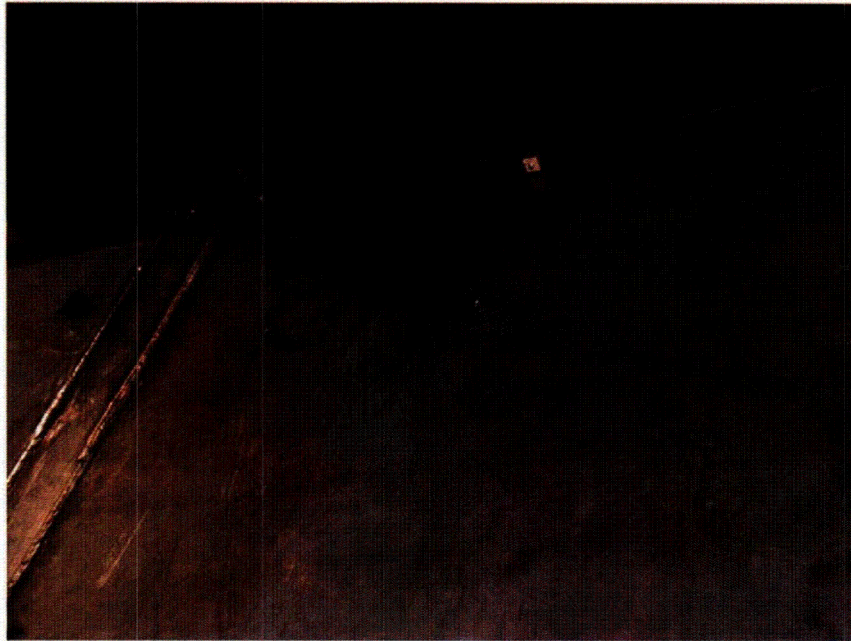


Figure 17: Response locations on upper part of left middle panel of 270 degree hood of Dryer #2



Figure 18: Response locations on upper part of right middle panel of 270 degree hood of Dryer #2

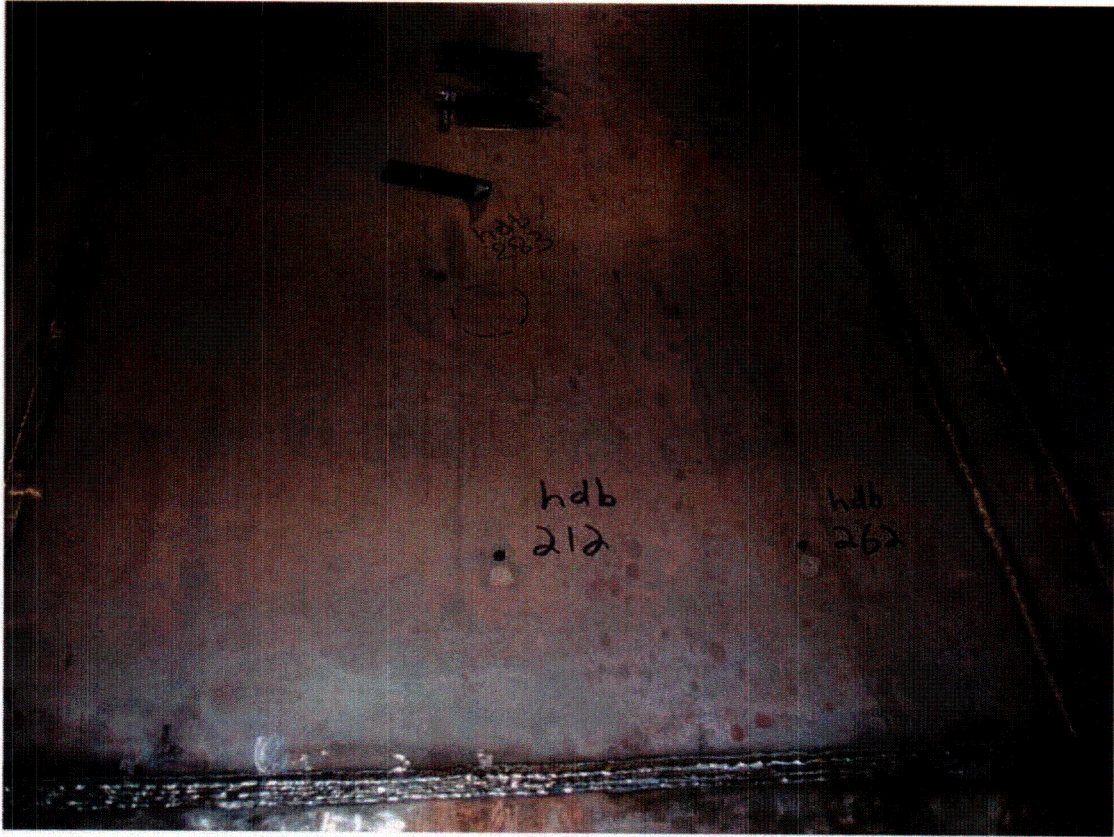


Figure 19: Response locations on lower part of right middle panel of 270 degree hood of Dryer #2

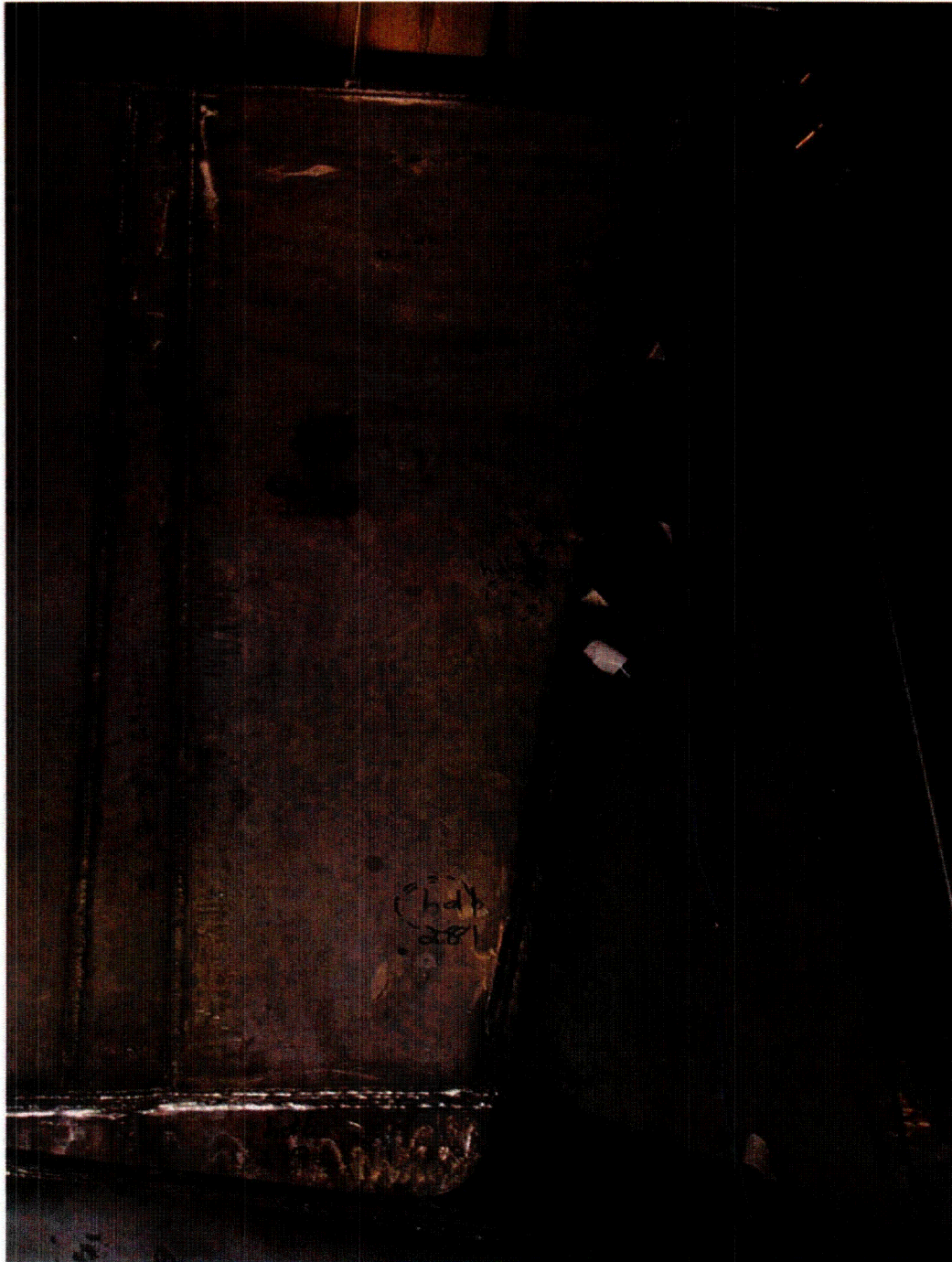


Figure 20: Response locations on rightmost panel of 270 degree hood of Dryer #2

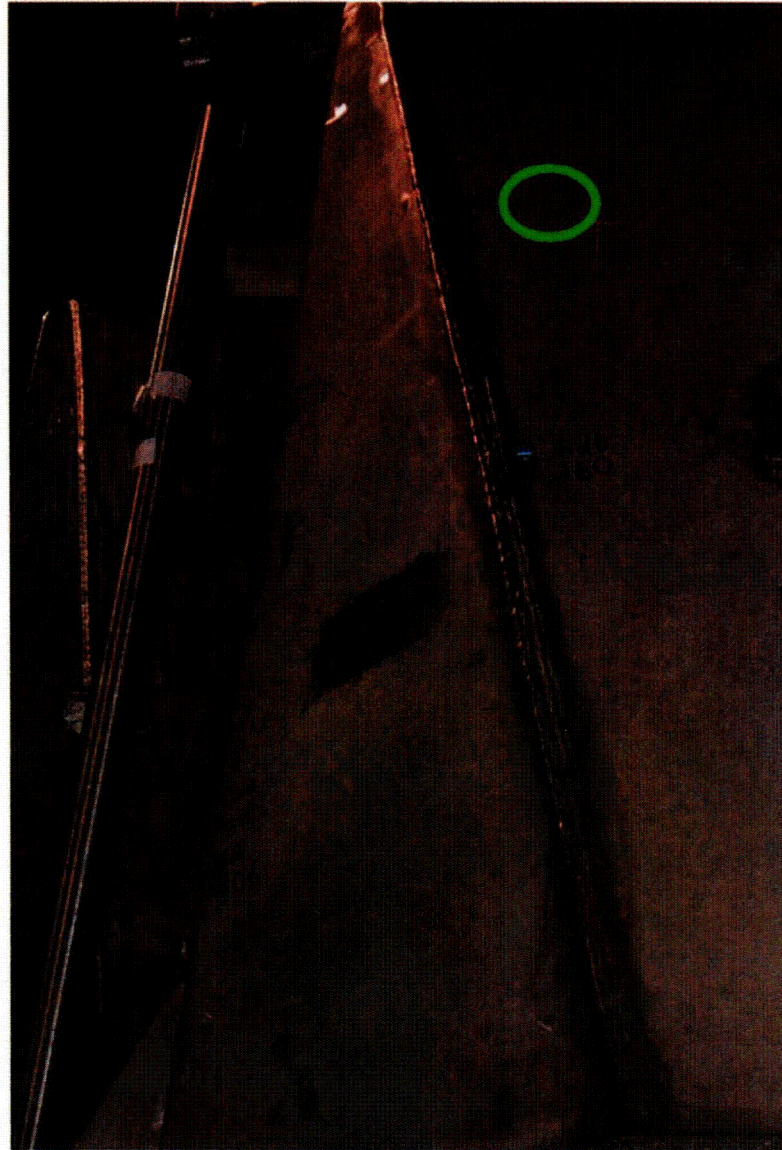


Figure 21: Response locations on side panel to the left of main panel of 270 degree hood of Dryer #2 (at angle with respect to main panel).

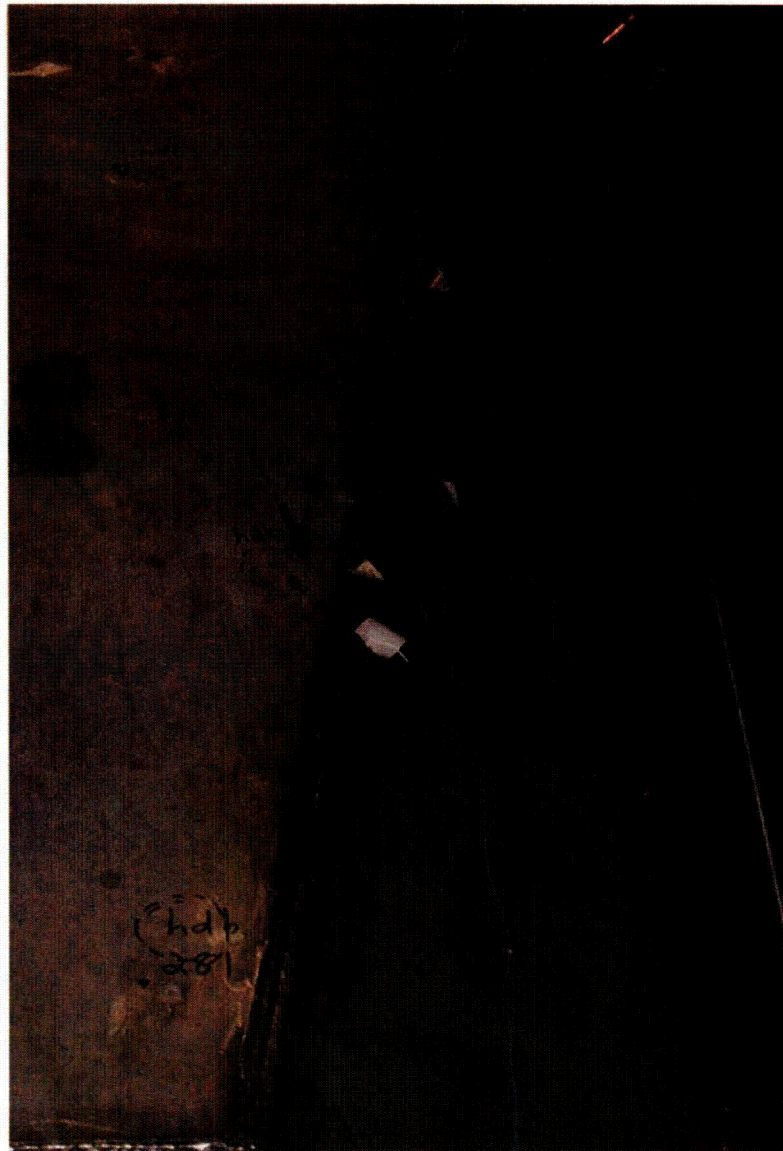


Figure 22: Response locations on side panel to the right of main panel of 270 degree hood of Dryer #2 (at angle with respect to main panel).

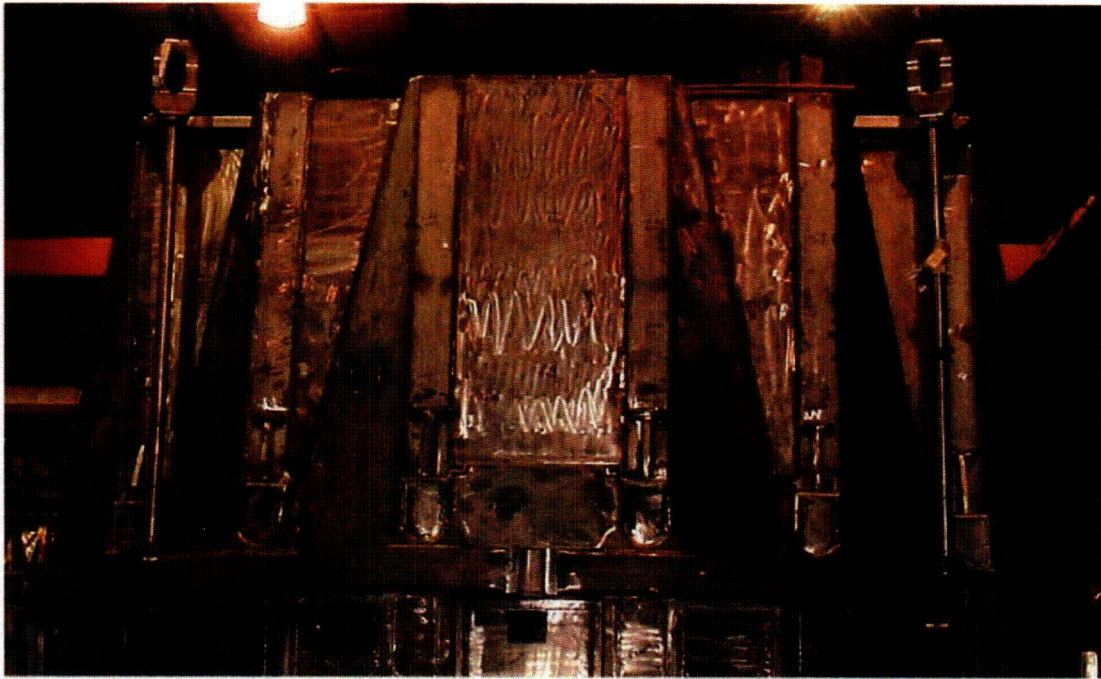


Figure 23: Full view of 0 degree side of Dryer #2 (before installation of temporary sensors).

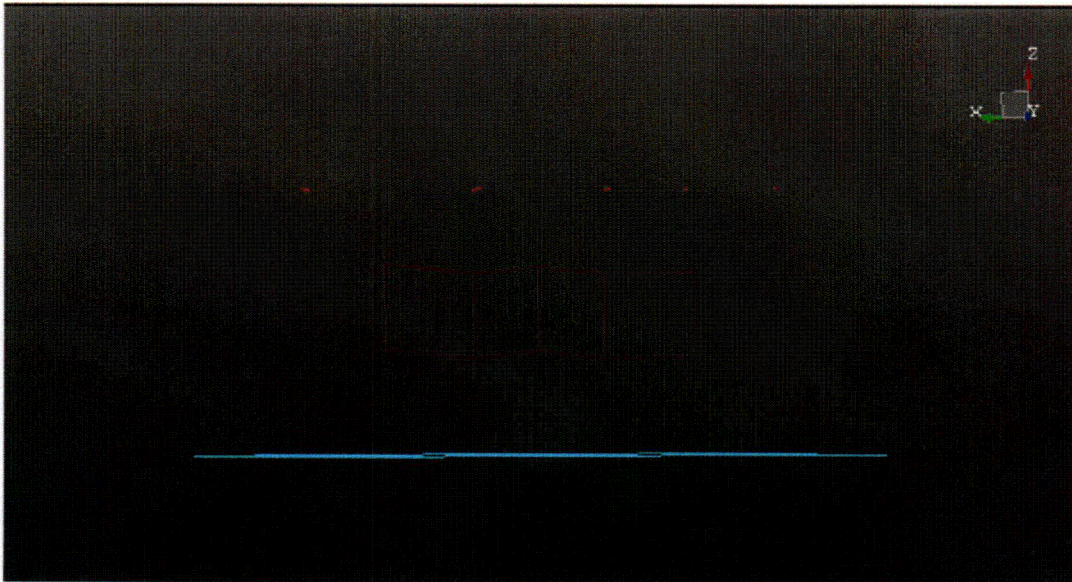


Figure 24: Pattern of measurement points for the 0 degree side of Dryer #2 where pink mesh is 0 degree side response locations, dark red is responses on top and aqua is responses on the ring.

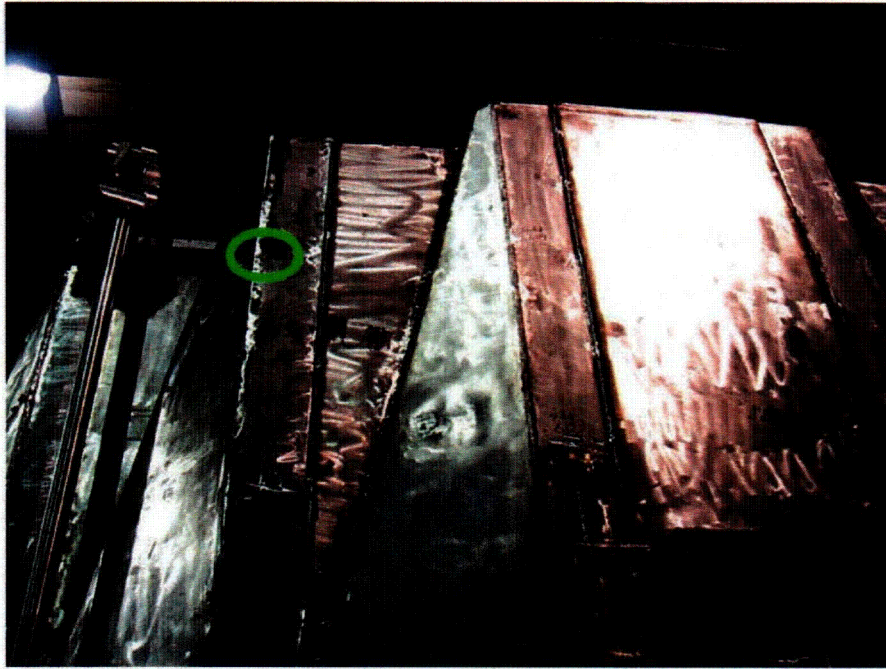


Figure 25: Response locations on left side of 0 degree side of Dryer #2 with green circle indicating one of input locations on 0 degree side

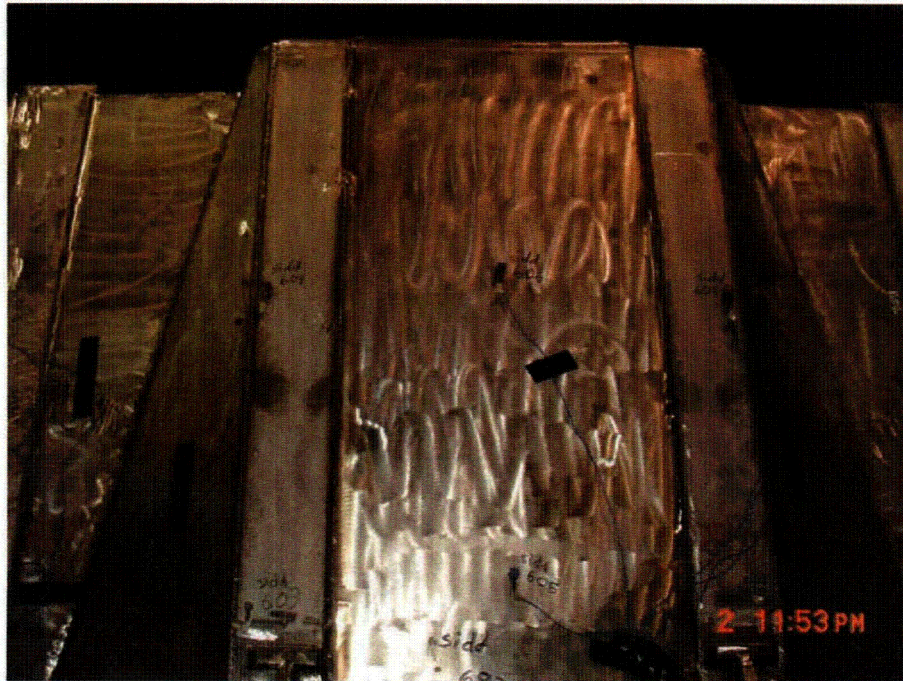


Figure 26: Response locations on middle section of 0 degree side of Dryer #2.

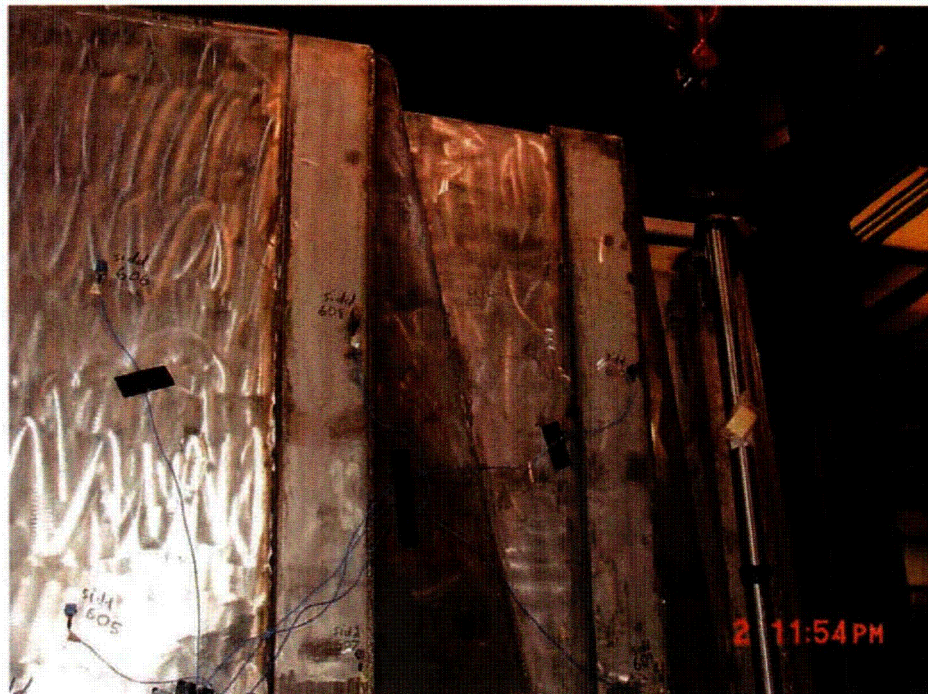


Figure 27: Response locations on right part of 0 degree side of Dryer #2.

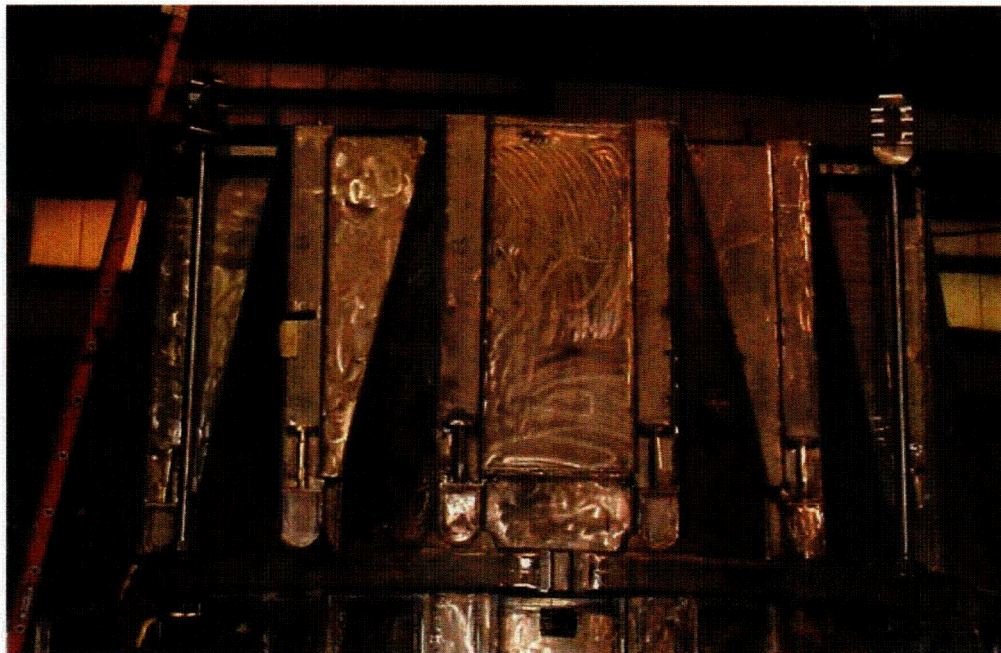


Figure 28: Full view of 180 degree side of Dryer #2 (before installation of temporary sensors).

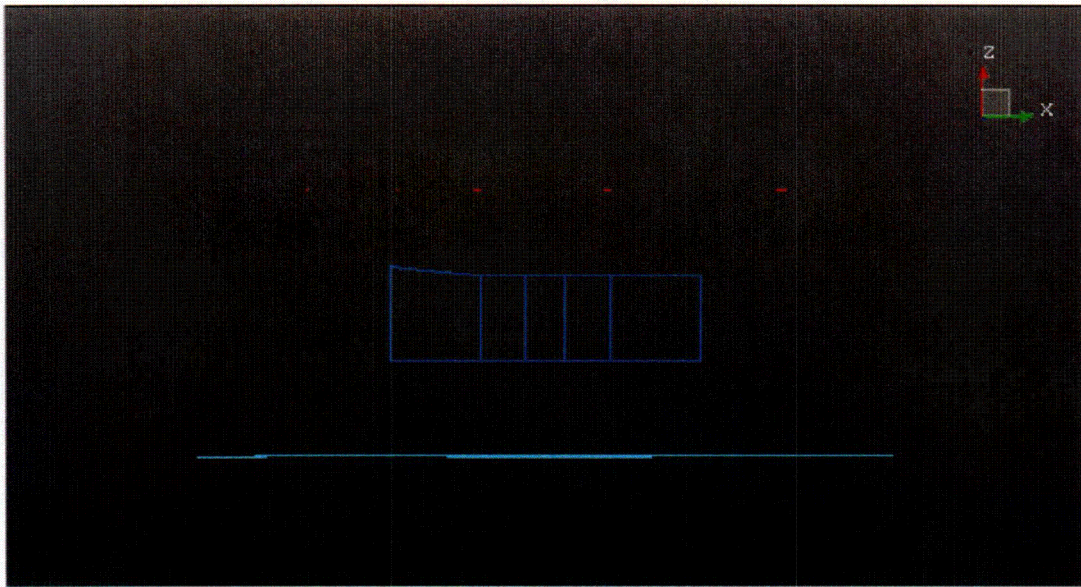


Figure 29: Pattern of measurement points for the 180 degree side of Dryer #2 where blue mesh is 180 hood response locations, dark red is responses on top and aqua is responses on the ring.

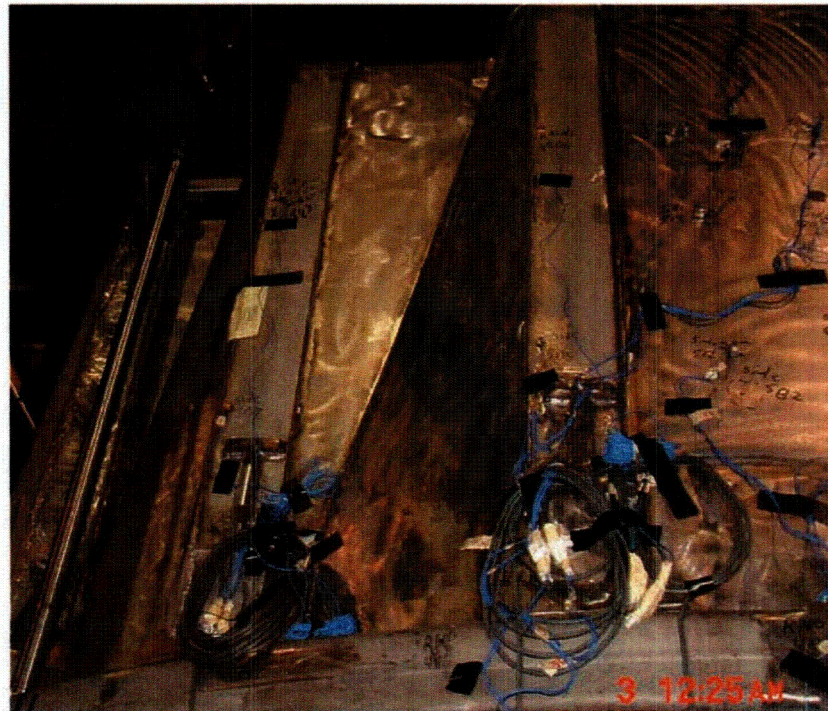


Figure 30: Response locations on left part of 180 degree side of Dryer #2.



Figure 31: Response locations on center section of 180 degree side of Dryer #2.



Figure 32: Response locations on right section of 180 degree side of Dryer #2.

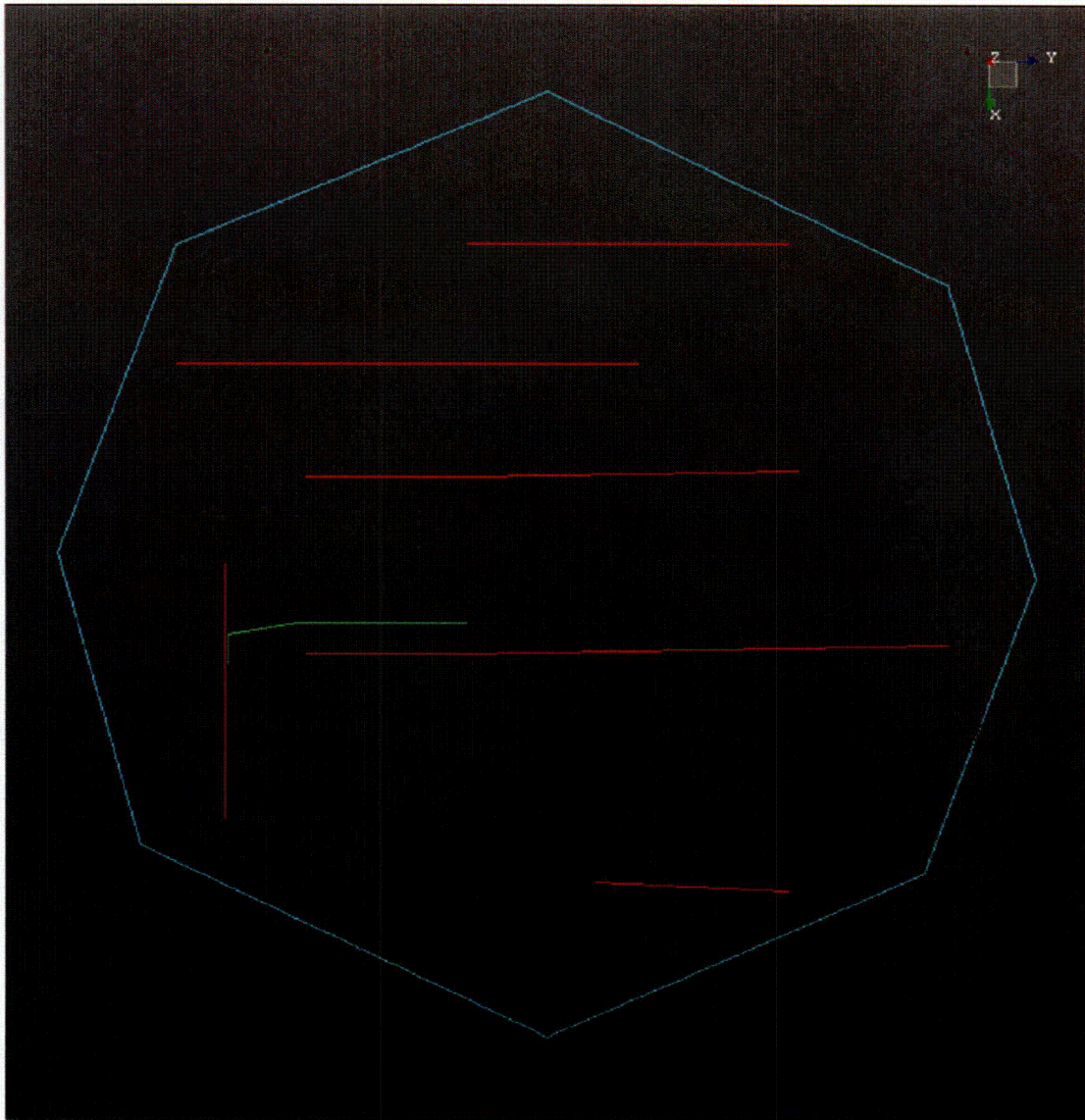


Figure 33: Pattern of measurement points for the top, tie bar and inner banks of Dryer #2 where maroon line is 0° side response locations, red is responses on top, pink is tie bar, green is inner bank/perforated panel responses and aqua is responses on the ring.



Figure 34: Response locations on top of Dryer #2, 0° to 90° quadrant

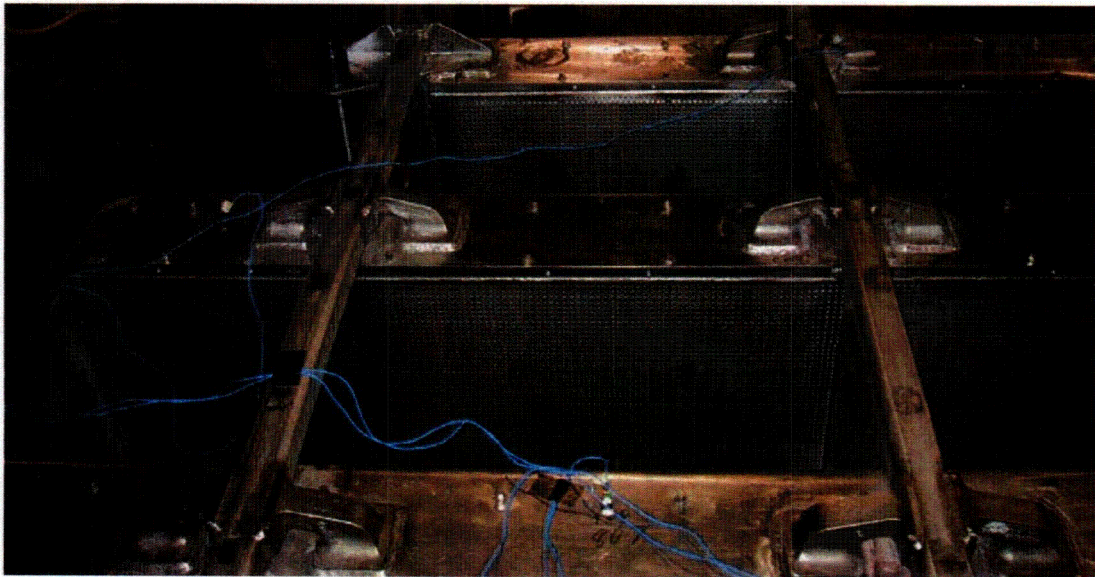


Figure 35: Response locations on top of Dryer #2, 90° to 180° quadrant

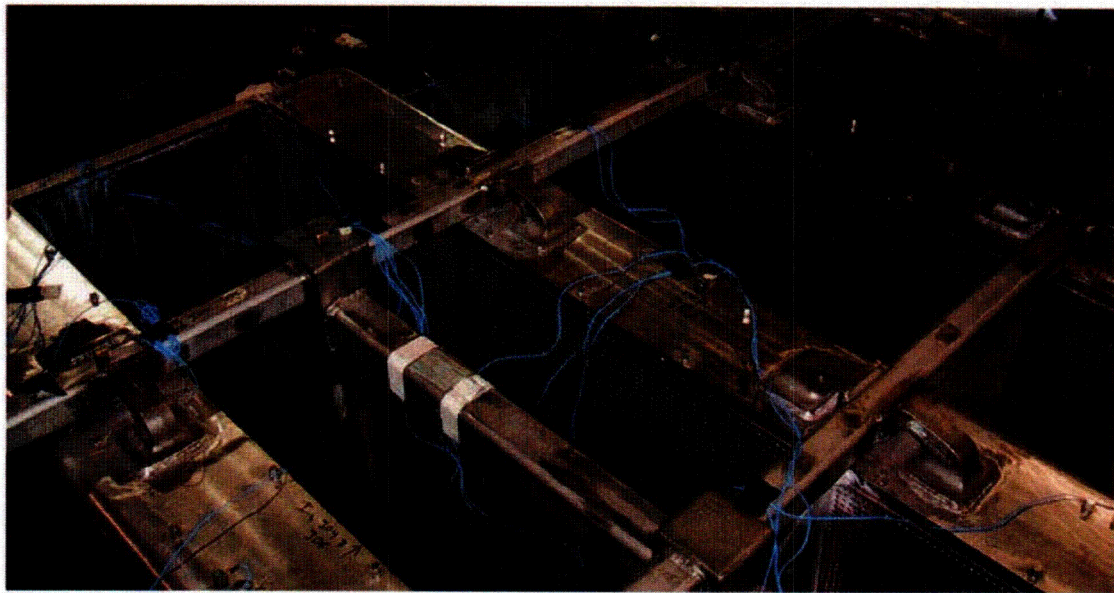


Figure 36: Response locations on top of Dryer #2, 180° to 270° quadrant

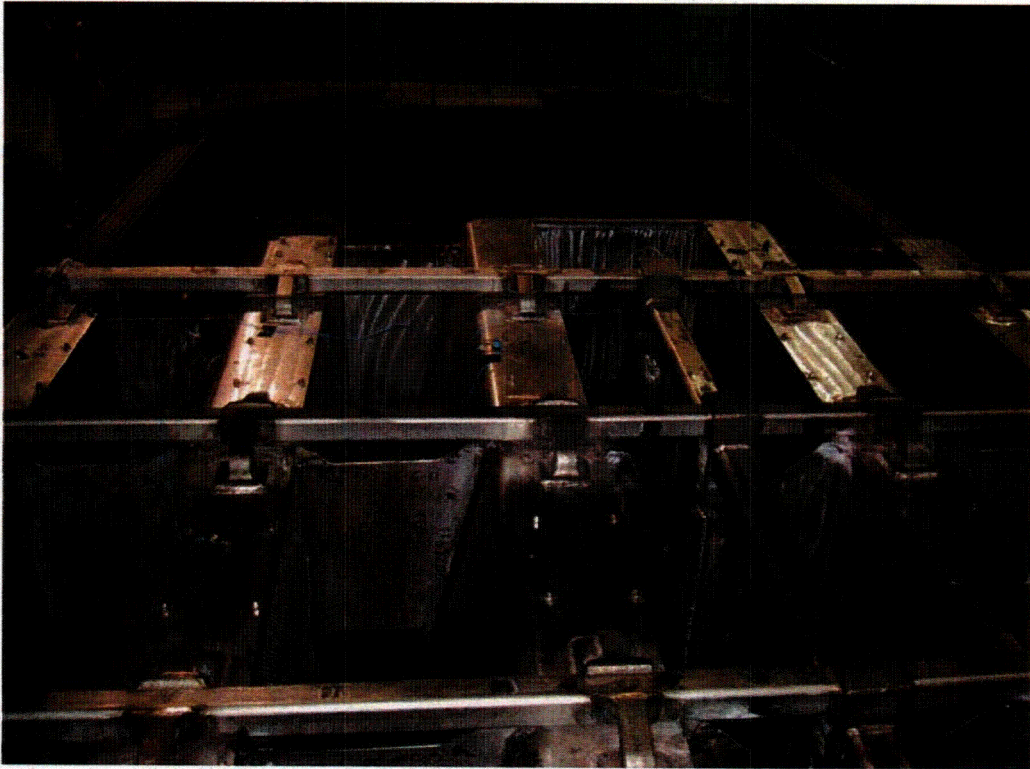


Figure 37 Response locations on top of Dryer #2, 270° to 0° region

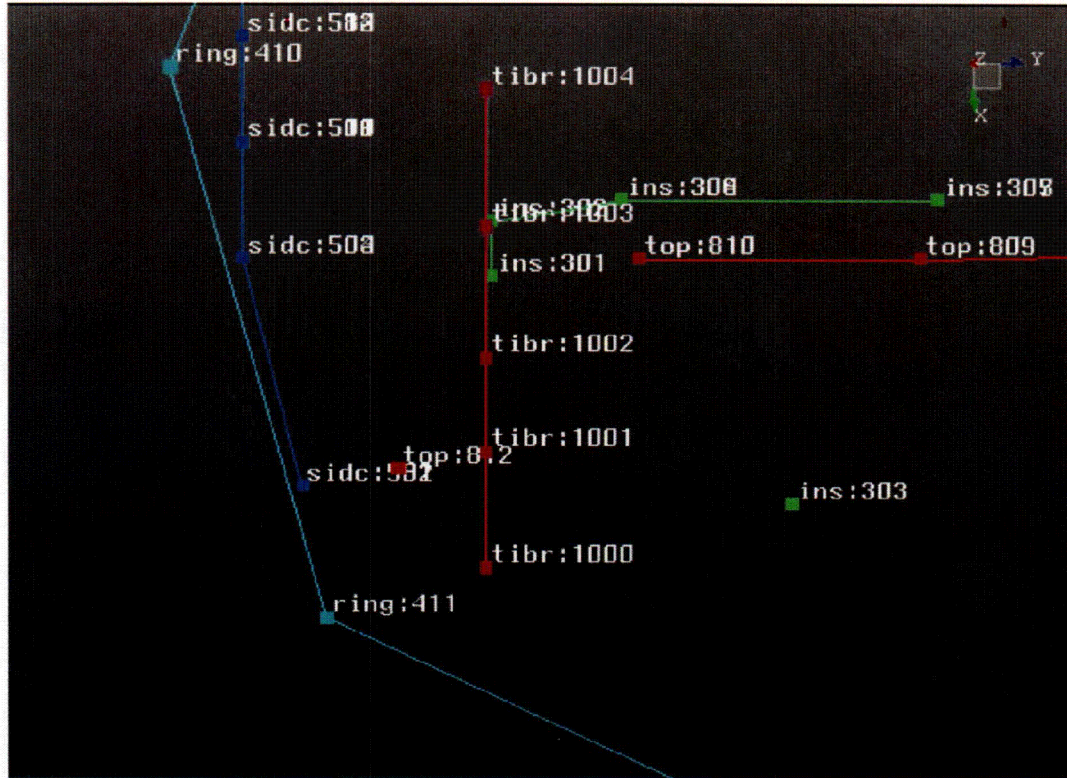


Figure 38: Close-up of Pattern of measurement points the top, tie bar and inner banks of Dryer #2 where blue mesh is 180 hood response locations, dark red is responses on top and aqua is responses on the ring.



Figure 39: Response locations on tie bar of Dryer #2

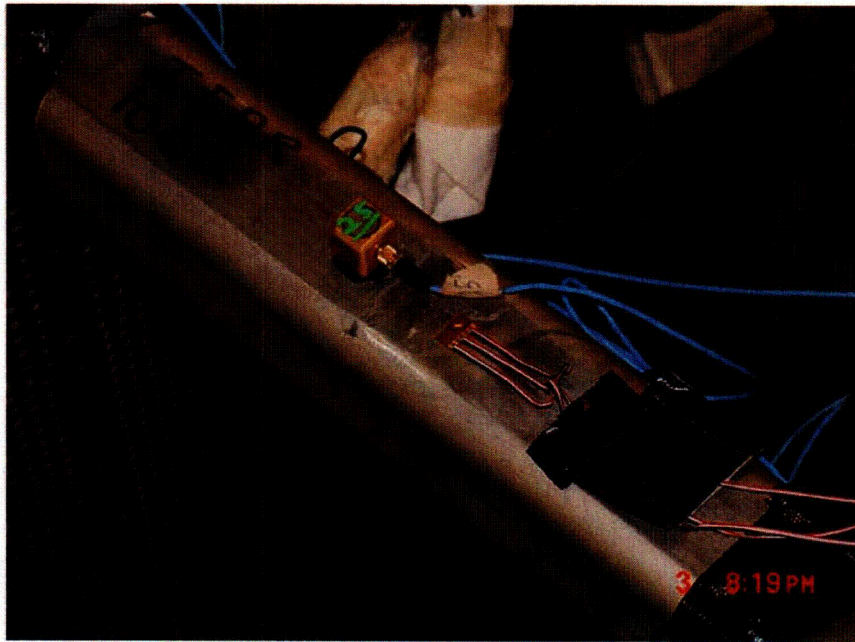


Figure 40: Strain Gage location on tie bar of Dryer #2 – Center gage of rosette was used

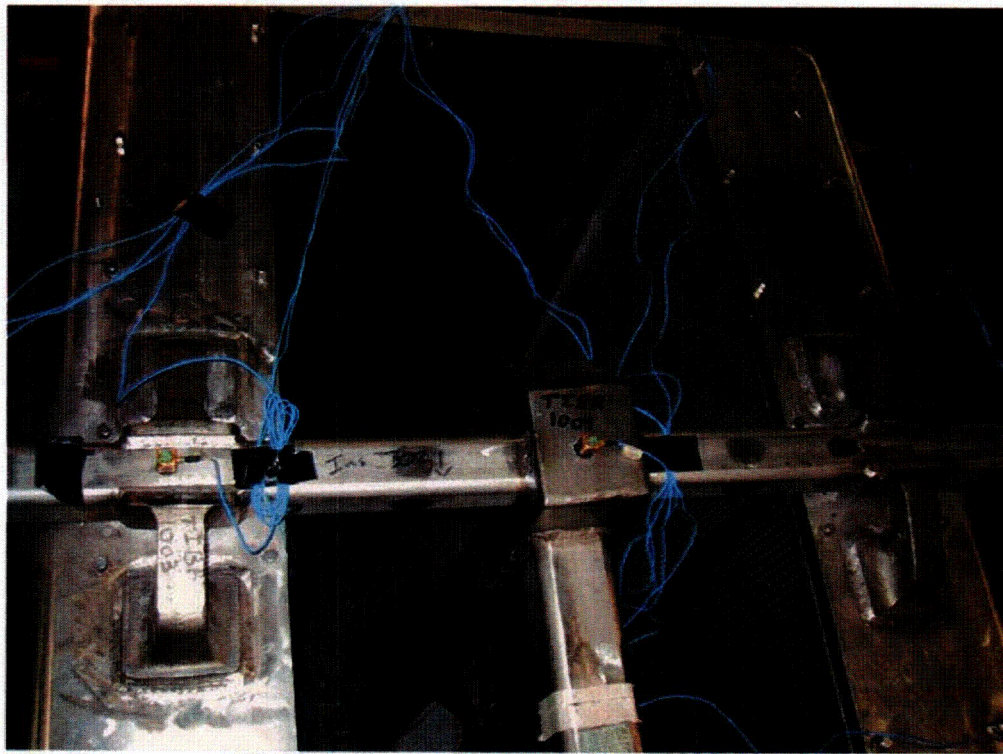


Figure 41: Response locations on tie bar of Dryer #2

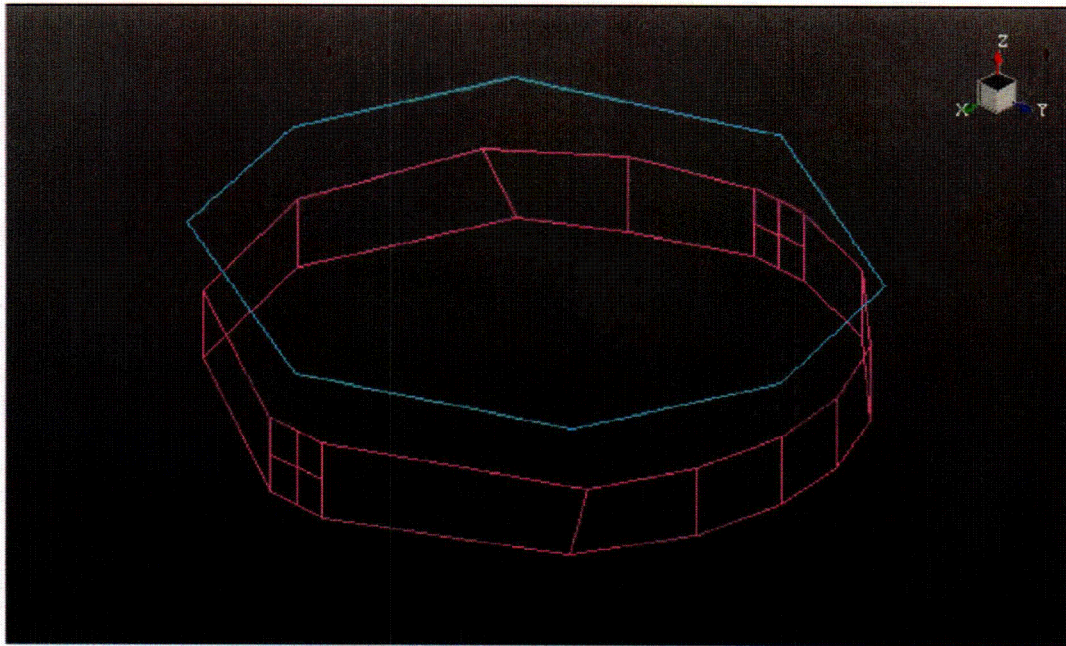


Figure 42: Pattern of measurement points for the skirt and ring of Dryer #2 where purple mesh is skirt response locations, and aqua mesh is the response locations on the ring.



Figure 43: Response locations skirt, 90° panel

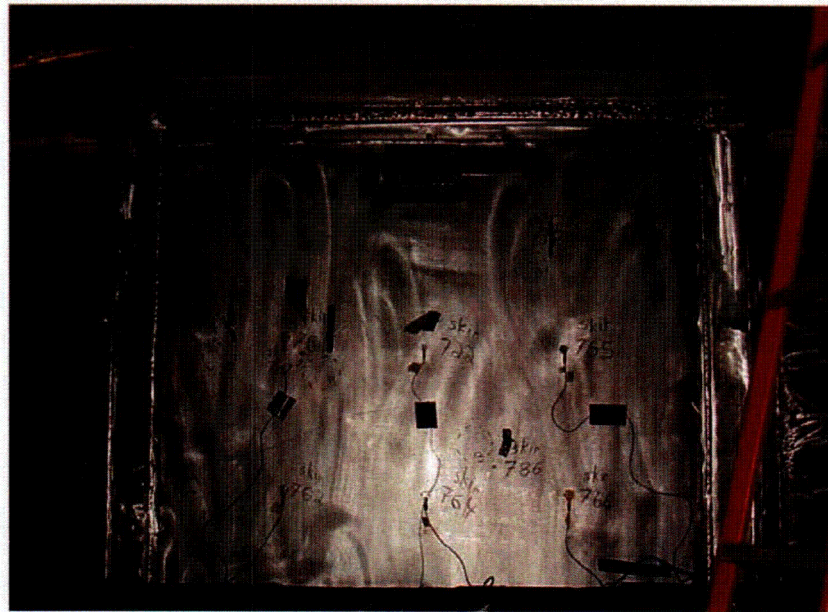


Figure 44: Response locations skirt, 270° panel

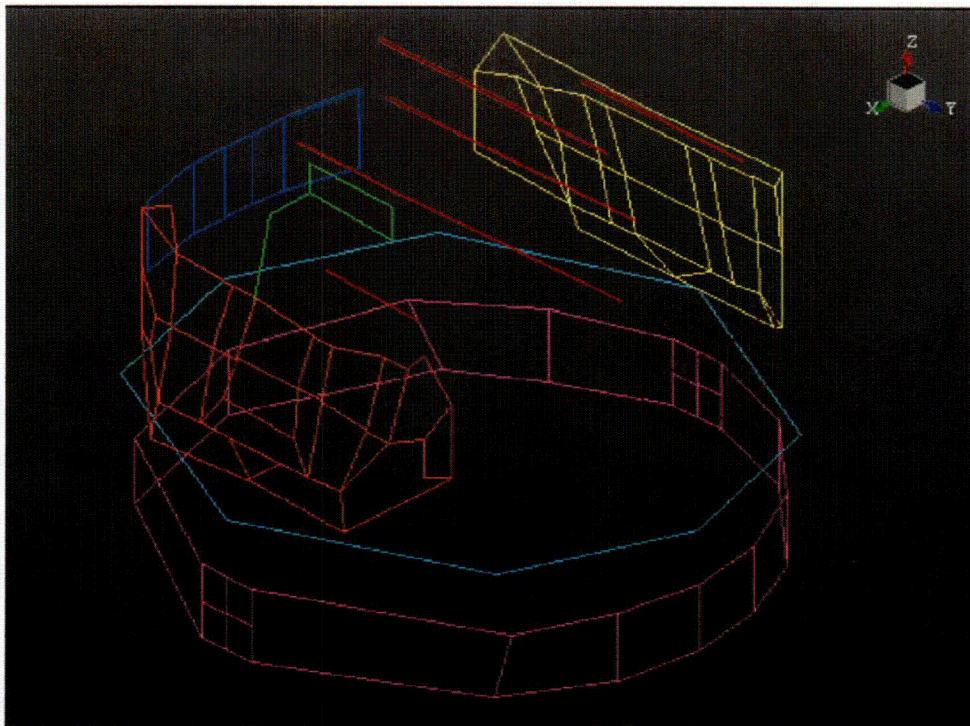


Figure 45: Pattern of measurement points for Dryer #2 where the red mesh is response locations on top, green is the response locations on the panels inside the dryer, aqua is responses on the ring, blue is responses on 180 degree side and pink is responses on 0 degree side.

[[

, .

Figure 46: Comparison of Damping levels from curve-fitting individual FRFs at Dry and LWL for Skirt
Panel Locations (Underwater at LWL)

[[

.

Figure 47: Comparison of Damping levels from curve-fitting individual FRFs at Dry and LWL for Skirt
Panel Locations (Underwater at LWL)

[[

,

,

]]

Figure 48: Summation FRF for Top: Red – Test

[[

]]

Figure 49: Summation FRF for 0° Side: Red – Test

[[

Figure 50: Summation FRF for Tie Bar: Red – Test

]]

[[

Figure 51: Summation FRF for Tie Bar – Extended Frequency Range: Red – Test

]]

||

Figure 52: Driving Point FRF (Strain Response) for Tie Bar at location of permanent sensor S6– Extended
Frequency Range: Red – Test

||

Figure 53: Summation FRF for Skirt: Red – FE, Green – Test Dryer #1, Blue – Test Dryer #2

[[

,

,

[[

Figure 54: Summation FRF for Skirt: Red – Test Containing all points

]]

Figure 55: Summation FRF for 90° Panel of Skirt: Red – Test Containing all 9 points

]]

[[

,

,

Figure 56: FRF on 90° Skirt Panel, Upper Point: Red – FE, Green – Test Dryer #1, Blue – Test Dryer #2

[[

Figure 57: FRF on 90° Skirt Panel, Lower Point: Red – FE, Green – Test Dryer #1, Blue – Test Dryer #2

[[

Figure 58: FRF on 90° Skirt Panel, Upper Point: Red –Test Dryer #1, Green – Test Dryer #2 (different input point than previous 2 figures)

[[

Figure 59: MAC Matrix for Skirt, [[

]]

]]

[[

Figure 60: Mode Shapes for Skirt, Local View: Left - [[]] Right - [[]]

[[

Figure 61: FE Mode Shape for Skirt [[]]

[[

,

,

Figure 62: MAC Matrix for Skirt, [[

]]

]]

[[

Figure 63: Mode Shapes for Skirt, Local View: Left – [[]], Right – [[]]

[[

Figure 64: FE Mode Shape for Skirt [[]]

[[

Figure 65: Mode Shapes for Skirt, Local View: Left – [[]] Right – [[]]
[[]]

Figure 66: FE Mode Shape for Skirt [[]]
]]

[[

]]

Figure 67: Summation FRF for 270° Panel of Skirt: Red – Test Containing all 9 points

[[

]]

Figure 68: FRF on 270° Skirt Panel, Upper Point: Red – FE, Green – Test Dryer #1, Blue – Test Dryer #2

[[

Figure 69: FRF on 270° Skirt Panel, Lower Point: Red – FE, Green – Test Dryer #1, Blue – Test Dryer #2]]

[[

Figure 70: FRF on 270° Skirt Panel, Lower Point: Red – Test Dryer #1, Green – Test Dryer #2 (different input point than previous 2 figures)]]

[[

Figure 71: Mode Shapes for Skirt, Local View: Left – [[

]] Right – [[

]]
]]

[[

Figure 72: Mode Shapes for Skirt, Local View: Left – [[]]
[[]]

Figure 73: FE Mode Shape for Skirt [[]]

[[

Figure 74: Mode Shapes for Skirt, Local View: Left – [[

]] Right – [[

]]
]]

[[

Figure 75: Summation FRF for 90°Hood: Red – FE, Green – Test Dryer #1, Blue – Test Dryer #2

[[

Figure 76: Mode Shapes for 90° Hood, Local View: Left – [[]] Right – [[]]

[[

Figure 77: Mode Shapes for 90° Hood, Local View: Left – [[]] Right – [[]]

[[

Figure 78: MAC Matrix for 90° Hood, [[]]

Figure 79: Mode Shapes for 90° Hood, Local View: Left – Test, [[]]

[[

Figure 80: Summation FRF for 270° Hood: Red – FE, Green – Test Dryer #1, Blue – Test Dryer #2]]

[[

Figure 81: Mode Shapes for 270° Hood, Local View: Top – [[]]
]] Bottom – [[]]

[[

]]

Figure 82: MAC Matrix for 270° Hood, [[

]]

[[

Figure 83: Mode Shapes for 270° Hood, Local View: Right – [[

]] Left – [[

]]
]]

Attachment A: Test Plan

General Electric Steam Dryer Experimental Modal and Static Load Test

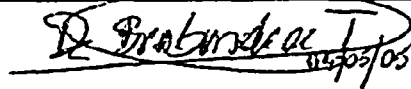
Hammer Test Plan

Procedure # GESD050505D2
Revision 5

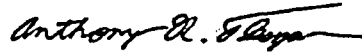
GE Purchase Order #431003474

Written By: Mike Neilheisel _____ Date: 04 May 2005

Reviewed By: Tom De Brabandere _____ Date: 04 May 2005


04/05/05

Approved By: Tony Fleszar _____ Date: 05 May 2005

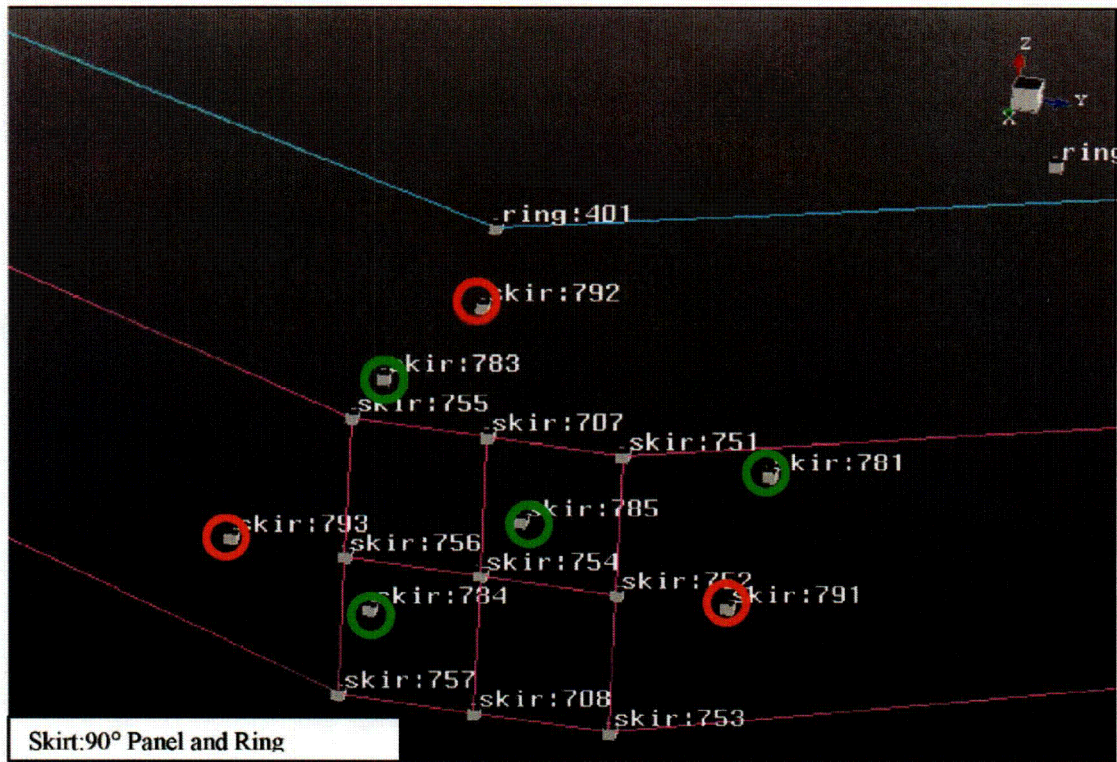


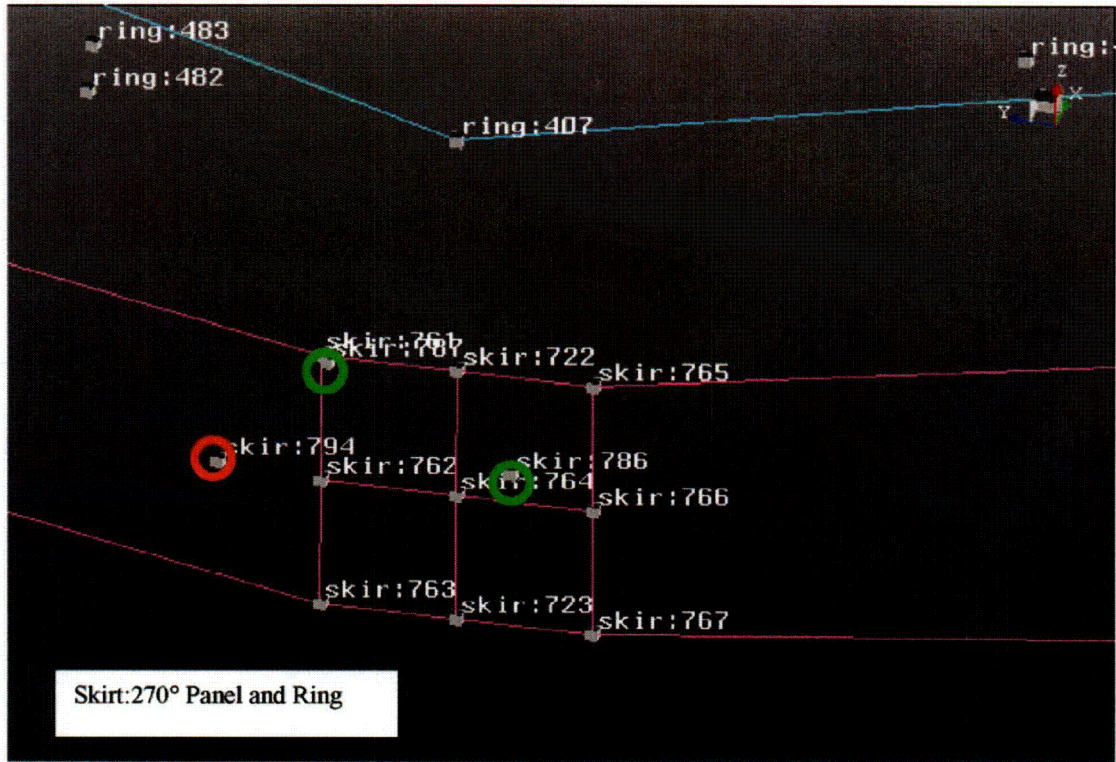
GENE-0000-0041-1656-01, Revision 2
Non-proprietary Version

1. Geometry - node selection and preparation
 - a.) 2 people
 - b.) Can be done while other work is done on dryer
 - c.) Marking of measurement locations for accelerometers and strain gages
 - d.) Cleaning of accelerometer and strain gage locations
 - e.) can be done while some other work is done on dryer (work that is not interfered with by cable routing or accelerometer position)
 - f.) Accelerometer locations will be those locations used for Dryer #1 as well as additional accelerometer locations determined by PreTest, information/requests from Structural Analysis Group, and lessons learned on first dryer
 - g.) GE to supply markers allowed to be used on dryer
2. Equipment setup (PC, front end and cables not on dryer itself)
 - a.) 2 people
 - b.) can be done while other work is done on dryer
 - c.) End-to-end measurement chain checks
3. Equipment Setup (cables on dryer)
 - a.) 2 people
 - b.) can be done while other work is done on dryer as long as other work is not interfered with by cable routing
4. Attachment of initial accelerometer set and of strain gages
 - a.) 1 person or 2 people focus on accelerometers
 - b.) 1 person focuses on strain gages (if strain gage attachment and wiring is not finished during this specific task it will continue while accelerometers are moved later)
 - c.) can be done while some other work is done on dryer (work that is not interfered with by cable routing or accelerometer position)
 - d.) Adhesive to be used is M-Bond 200 (a super glue with an accelerator) as it has been approved for use on the dryer
 - e.) Solvent will be acetone as it is approved for use on the dryer
 - f.) Sandpaper is Silicon Carbide paper in strain gage kit
 - g.) Initial set of accelerometers focuses on skirt (additional points added to 90° and 270° skirt panels since Dryer #1 modal)
5. Frequency Response Function (FRF) Measurements/Hammer Impact Testing
 - a.) Re-verify that all transducers are operational
 - b.) Verify acceptability of excitation locations (3 global excitation locations and a minimum of 3 excitation locations for each component)
 - c.) Perform initial set of measurements dry (Current plan is to have 35 to 38 triaxial accelerometers, 1 impact hammer, and 1 single-axis driving point accelerometer in each set. 90° Skirt Panel will have 3 rosette strain gages, 270° Skirt Panel will have 1 rosette strain gage, 270° hood will have 2 rosette strain gages and tie bar will have 1 single axis strain gage at point determined by GE. Underwater accels will be distributed as follows: 2 on drain channels [1 on the S1/S2 drain channel], and 3 on skirt panels).
 - d.) Add water to reach Lower Water Level (LWL)
 - e.) Perform LWL measurement on 1st set (focus on skirt)
 - f.) Perform special drain channel test at LWL. Impact the drain channel with the hardest tip on the modal sledge or use the hand sledge to excite the drain channel modes to at least 400 Hz. Data will require review to see if it needs to be excited to 800 Hz.

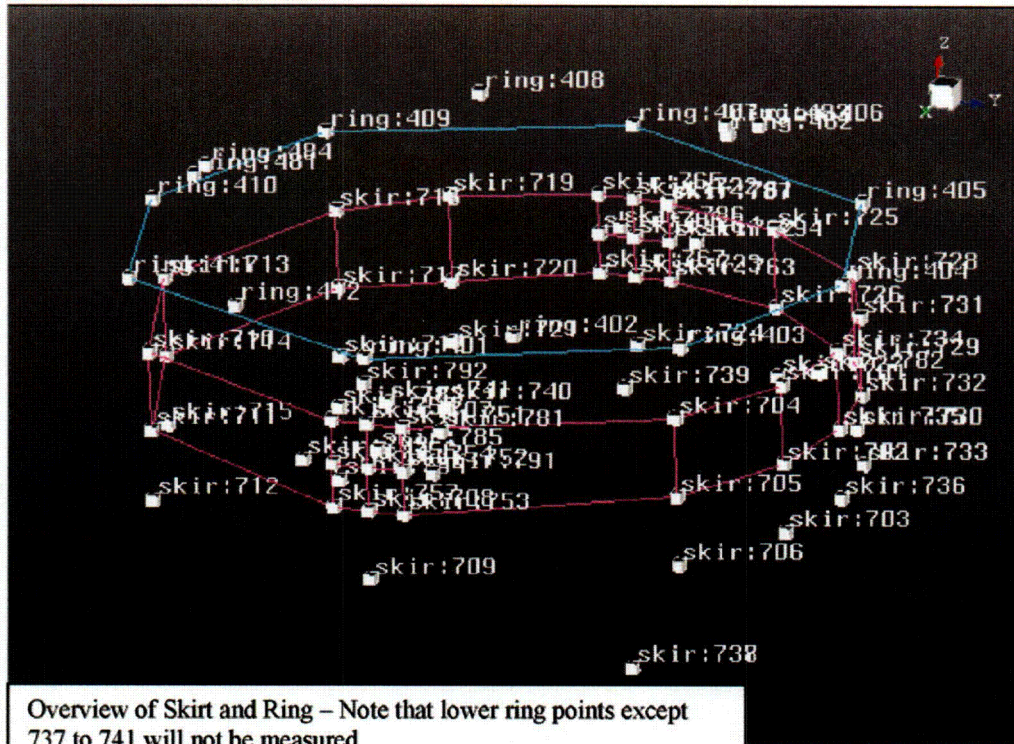
GENE-0000-0041-1656-01, Revision 2
Non-proprietary Version

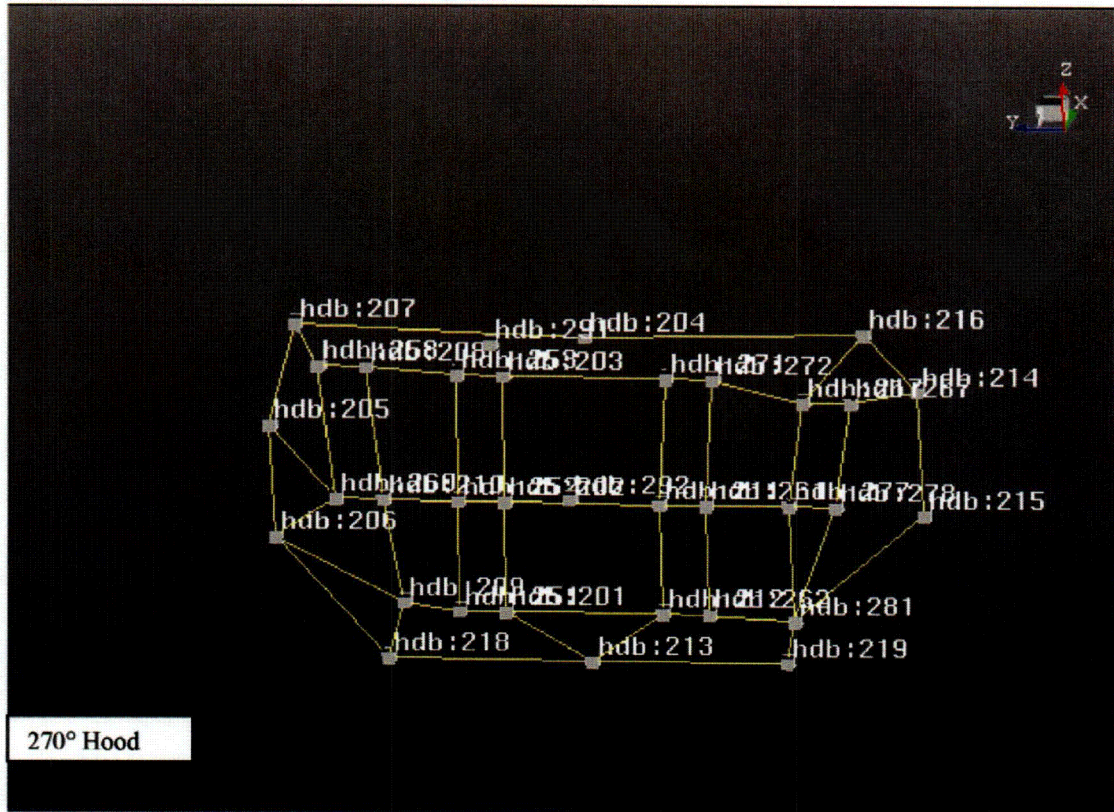
- g.) Move cables to next accelerometer set.
- h.) Perform 2nd set at LWL (focus on 270° hood)
- i.) Perform additional damping measurements on 2nd set at LWL
- j.) Drain tank to dry while moving 1st set of accelerometers
- k.) Perform 2nd set at dry (focus on 270° hood)
- l.) Perform 3rd set at dry (focus on 90° hood)
- m.) Add water to reach LWL while moving 2nd set of accelerometers
- n.) Perform 3rd set at LWL (focus on 90° hood)
- o.) Perform additional damping measurements on 3rd set at LWL
- p.) Move cables to next accelerometer set.
- q.) Perform 4th set at LWL (focus on 0° and 180° sides, ring and supports)
- r.) Drain tank to dry while moving 3rd set of accelerometers
- s.) Perform 4th set at dry (focus on 0° and 180° sides, ring and supports)
- t.) Move cables to next accelerometer set
- u.) Perform 5th set at dry (focus on top, inner banks and tie bar)
- v.) Add water to reach LWL while moving accelerometers to repeat points as necessary or perform additional measurements
- w.) Perform 5th set at LWL
- x.) Perform additional measurements on tie bar with strain gage at permanent sensor location (see Item 6)
- y.) Perform additional damping measurements on strain gages and reduced set of accelerometers from 1st set at LWL (Included here for timing purposes - see Item 6)
- z.) Perform additional damping measurements on reduced set of accelerometers from 2nd set at LWL (Included here for timing purposes - see Item 6)
- aa.) Perform additional damping measurements on strain gages and reduced set of accelerometers from 3rd set at LWL (Included here for timing purposes - see Item 6)
- bb.) Perform additional set at LWL if necessary (points where repeat is necessary or additional points)
- cc.) Drain water
- dd.) Perform additional set at dry if necessary
- cc.) The following pictures show the proposed excitation locations as green circles or ovals, the accelerometer response locations as dots and the strain gage response locations as dots surrounded by orange circles. The proposed excitation locations are shown only on the zoomed in views.



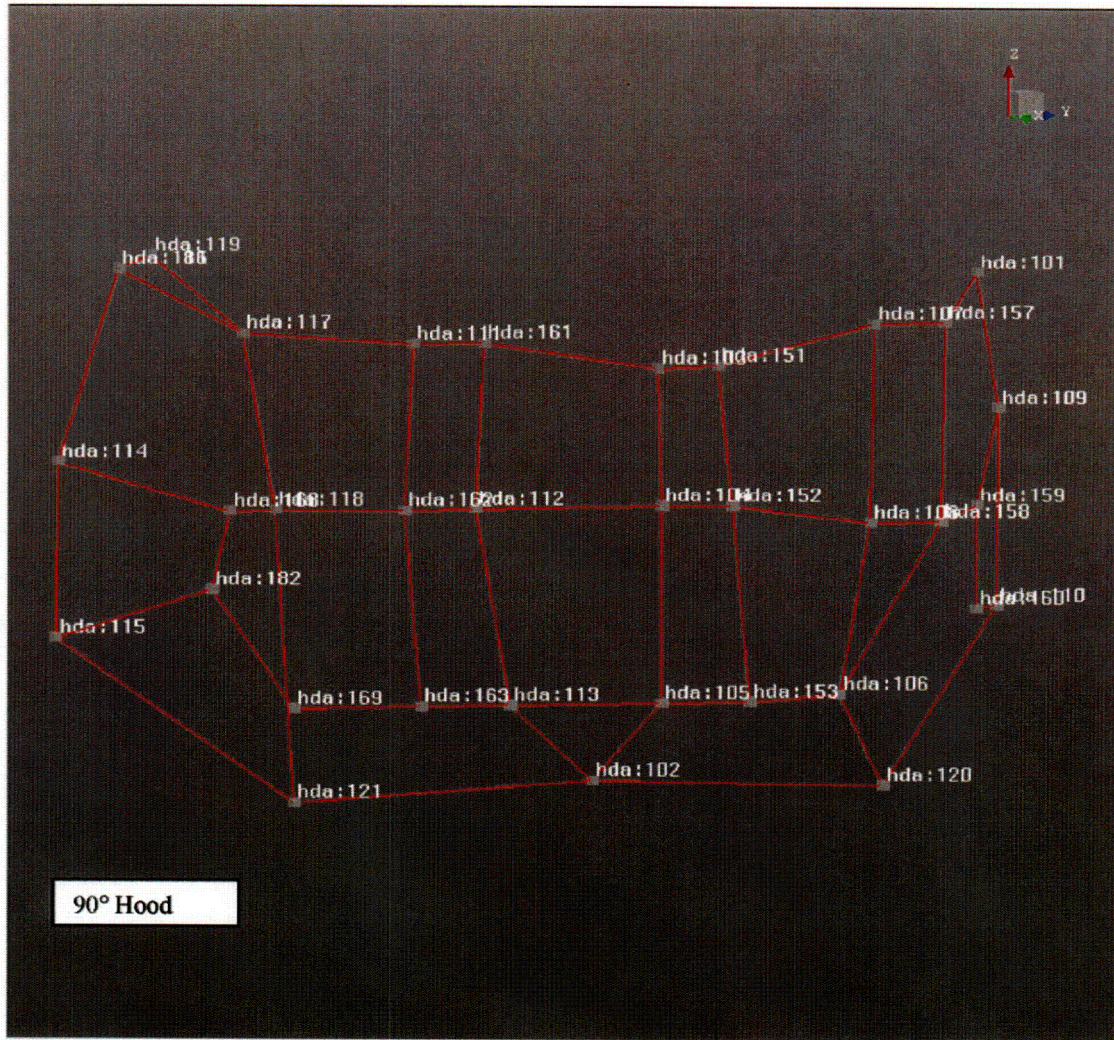


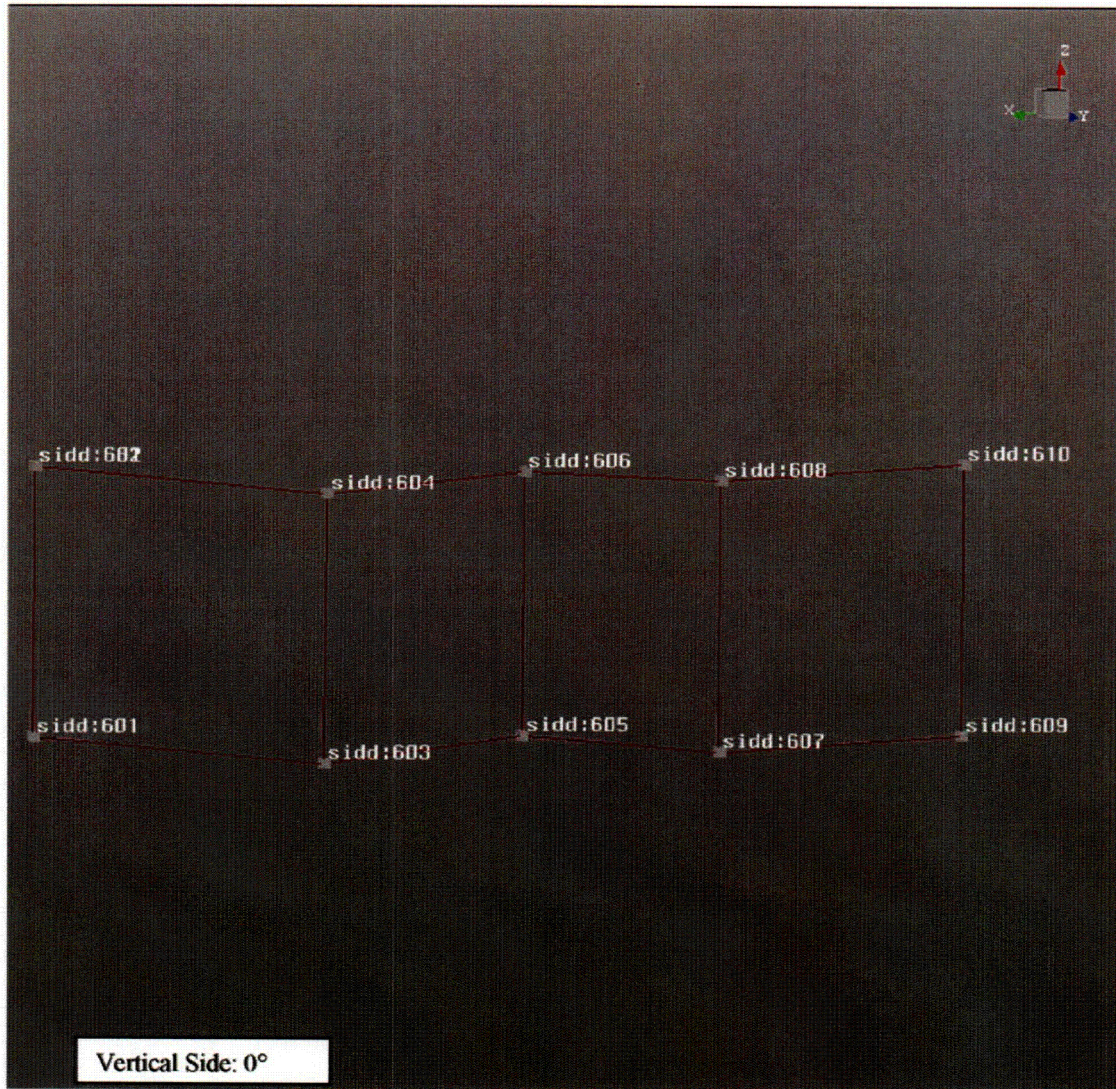
GENE-0000-0041-1656-01, Revision 2
Non-proprietary Version



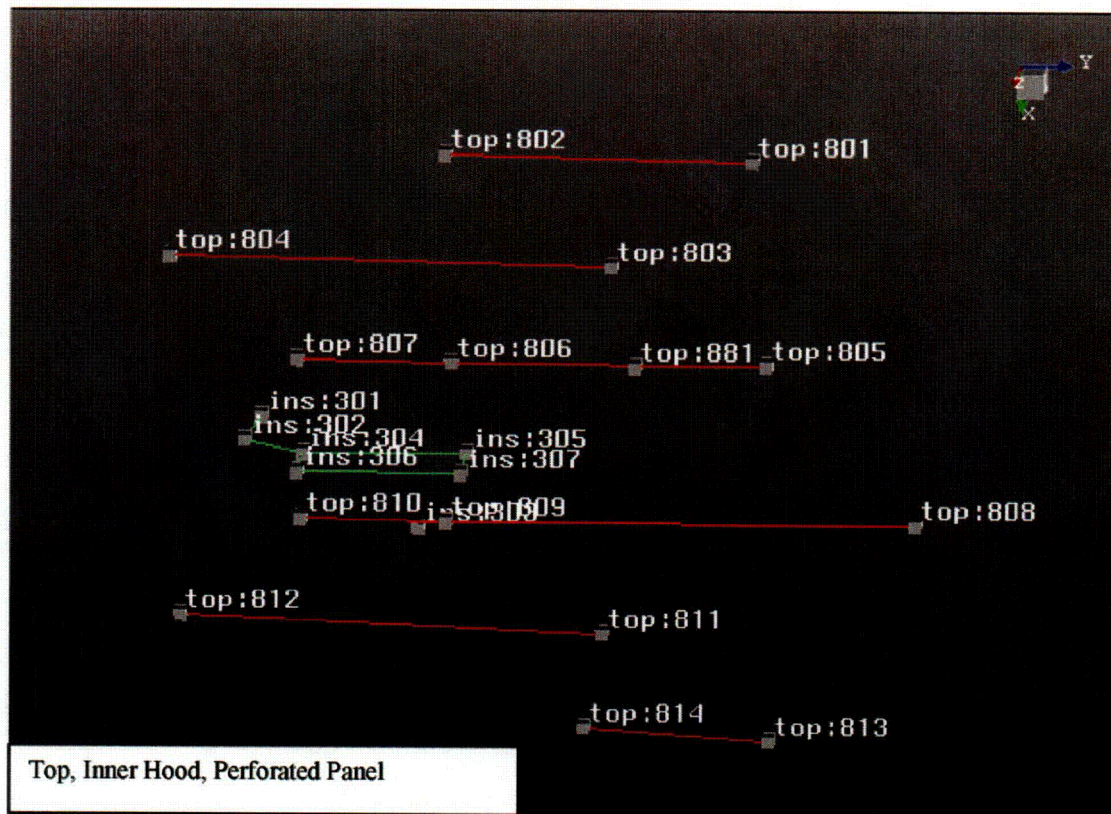


GENE-0000-0041-1656-01, Revision 2
Non-proprietary Version









Data checks include but are not limited to:

- a.) Review of input time records for input force and acceleration response during data acquisition
- b.) Review of Input Autopower
- c.) Review of FRF and coherence for each location (specific review of driving point)
- d.) Reciprocity check
- e.) Repeatability of driving point measurements among sets
- f.) After checks for each set are done, frequency content will be available for that set
- g.) As sets are performed, preliminary curve-fitting will be performed to check data and to obtain damping results

6. **Special Strain Gage and Time Domain Testing: 2 to 3 people, no other work done on dryer**

- a.) Apply strain gages to the 90° skirt panel and 270° skirt panel, to the 90° outer hood (the same locations on the 90° outer hood as used for the static load test), and to the tie bar.
- b.) Perform both FRF measurements and time domain responses to impacts using at least some but not necessarily all of the input points on the specific component being tested

GENE-0000-0041-1656-01, Revision 2
Non-proprietary Version

7. **Static load testing: 3 people, no other work done on dryer**
 - a.) 3 people
 - b.) Apply 1000 lb. load with hydraulic jack (assistance from GE/USTD required for providing backstop for jack), measure strain on 90° hood using 2 rosette strain gages or 1 rosette strain gage and 1 assembly of 2 strain gages
 - c.) Load application location – 90° outer hood near MSL nozzle location – still being reviewed as are strain gage locations

8. **Final hammer impact measurements if necessary**
 - a.) 2 or 3 people
 - b.) Repeat any points where data was inadequate for any reason or add additional points as determined by review during data acquisition (added points on perforated panels on inner banks, on support lug, and near support locations).
 - c.) Perform driving point measurements at support locations if not incorporated in earlier sets
 - d.) Would be determined by analysis and processing done along way and data review while static load testing is performed

9. **Removal of accelerometers and cables on dryer**
 - a.) 2 or 3 people
 - b.) can be done while some other work is done on dryer (work that is not interfered with by cable routing or accelerometer position)
 - c.) Discussion will occur with GE about timing. If it makes sense, 1 person will continue processing data while 1 or 2 others remove accelerometers based on need to make dryer available.

10. **Surface cleanup**
 - a.) 2 or 3 people
 - b.) can be done while other work is done on dryer
 - c.) May be left to later depending on schedule

11. **Equipment breakdown (PC, front end and cables not on dryer)**
 - a.) 2 or 3 people
 - b.) can be done while other work is done on dryer

12. **Model Solution**
 - a.) Separate from work on dryer
 - b.) Receive model from GE and review
 - c.) Solve model – first attempt full modal analysis
 - d.) If modal analysis not feasible, perform modal superposition to obtain FRFs at same input and response points as used in experimental modal analysis
 - e.) Also perform modal analysis in frequency bands to obtain output file sizes that can be handled

GENE-0000-0041-1656-01, Revision 2
Non-proprietary Version

- 13. Damping Calculations**
 - a.) Perform damping calculations on skirt panels using modal curvefitting on accelerometer and strain gage data
 - b.) Perform damping calculations on hoods using modal curvefitting on accelerometer and strain gage data.

- 14. Experimental Modal Analysis Processing**
 - a.) Review data sets – generate sets of clean data
 - b.) Perform processing to obtain global mode shapes, frequencies and damping
 - c.) Perform processing on specific components to focus in on component mode shapes, frequencies and damping

- 15. Comparison of Experimental Modal Analysis Results to Finite Element Results**
 - a.) Compare FRF measurements between test and FE
 - b.) Generate summation FRFs on a component basis, and compare between test and FE
 - c.) Use summation FRFs to attempt to define similar peaks between test and FE
 - d.) Perform MAC calculations on a global basis
 - e.) Perform MAC calculations on a component basis
 - f.) Visually compare mode shape animations between test and FE based on summation FRFs and MAC results.
 - g.) Compare Dryer 1 to Dryer 2 results

Attachment B: Hammer Tip Study

Figures B-1, B-2 and B-3 are comparisons of the softest tip with the medium tip for measurements on Dryer#1 with no water. The softest tip provides better low frequency results than the medium tip. The low frequency portion of the FRF is cleaner as seen in the middle plot in Figures B-1, B-2 and B-3, and the low frequency portion of the coherence, the lower plot in Figure B-1, B-2 and B-3, has a higher value with the softest tip. At the start of testing on Dryer #1, it was believed that obtaining very good low frequency data was more important than extending the frequency range of the results; however, subsequent review and discussion of the results produced a decision to use the medium tip for Dryer #2.

[[

]]
Figure B-1: Comparison of Measurements using Hammer Tips of different hardness, Radial Skirt Response to Radial Skirt Impact (Red curve is soft tip, Green curve is medium tip)

[[

]]
Figure B-2: Comparison of Measurements using Hammer Tips of different hardness, Vertical Side Response to Skirt Impact (Red curve is soft tip, Green curve is medium tip)

[[

]]

Figure B-3: Comparison of Measurements using Hammer Tips of different hardness, 90° Hood Response to Skirt Impact (Red curve is soft tip, Green curve is medium tip)

Attachment C: Effect of Number of Averages

GENE-0000-0041-1656-01, Revision 2
Non-proprietary Version

This attachment illustrates how the FRF measurement and coherence are affected when a different number of hammer impacts is used. Two measurements have been taken with the same excitation and response locations, one measurement with twenty hammer impacts and one measurement with five hammer impacts. The data presented in the following figures was measured on the 90 degree and 270 degree skirt panels of Dryer #2 (the dryer without permanent sensors intended for Quad Cities Unit # 1 (QC1)).

Specific measurements show some difference between 20 averages and 5 averages, particularly near [] These differences are attributed to inconsistency in the hammer impact. In general, the frequency, shape, and phase of the FRF are consistent between 20 averages and 5 averages. The phase of the FRF is generally "cleaner" with 20 averages as well. The coherence shows some differences between 20 averages and 5 averages, but the differences appear to be specific to individual measurements and usually at low frequency – below [] The other coherence differences are near [] and correspond to those measurements with some difference in FRF amplitude that has been attributed to inconsistency in the hammer impact.

[

]]
Figure C-1: Comparison of the FRF amplitude, FRF phase and coherence between a hammer impact measurement with 20 averages (red) and one with 5 averages (green) for normal excitation in point skir:785 and normal response in point skir:785 on the 90 degree skirt panel of dryer 2

[[

[[

Figure C-2: Comparison of the FRF amplitude, FRF phase and coherence between a hammer impact measurement with 20 averages (red) and one with 5 averages (green) for normal excitation in point skir:785 and normal response in point skir:753 on the 90 degree skirt panel of dryer 2]]

[[

Figure C-3: Comparison of the FRF amplitude, FRF phase and coherence between a hammer impact measurement with 20 averages (red) and one with 5 averages (green) for normal excitation in point skir:785 and vertical response in point skir:753 on the 90 degree skirt panel of dryer 2]]

[[

]]
Figure C-4: Comparison of the FRF amplitude, FRF phase and coherence between a hammer impact measurement with 20 averages (red) and one with 5 averages (green) for normal excitation in point skir:785 and lateral response in point skir:753 on the 90 degree skirt panel of dryer 2

[[

]]
Figure C-5: Comparison of the FRF amplitude, FRF phase and coherence between a hammer impact measurement with 20 averages (red) and one with 5 averages (green) for normal excitation in point skir:785 and normal response in point skir:707 on the 90 degree skirt panel of dryer 2

[[

]]
Figure C-6: Comparison of the FRF amplitude, FRF phase and coherence between a hammer impact measurement with 20 averages (red) and one with 5 averages (green) for normal excitation in point skir:785 and vertical response in point skir:707 on the 90 degree skirt panel of dryer 2

[[

]]
Figure C-7: Comparison of the FRF amplitude, FRF phase and coherence between a hammer impact measurement with 20 averages (red) and one with 5 averages (green) for normal excitation in point skir:785 and lateral response in point skir:707 on the 90 degree skirt panel of dryer 2

[[

]]
Figure C-8: Comparison of the FRF amplitude, FRF phase and coherence between a hammer impact measurement with 20 averages (red) and one with 5 averages (green) for normal excitation in point skir:785 and normal response in point skir:722 on the 270 degree skirt panel of dryer 2

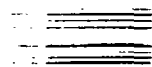
[[

]]
Figure C-9: Comparison of the FRF amplitude, FRF phase and coherence between a hammer impact measurement with 20 averages (red) and one with 5 averages (green) for normal excitation in point skir:785 and normal response in point skir:762 on the 270 degree skirt panel of dryer 2

||

Figure C-10: Comparison of the FRF amplitude, FRF phase and coherence between a hammer impact measurement with 20 averages (red) and one with 5 averages (green) for normal excitation in point skir:785 and response in strain gage channel C in point skir:796 on the 90 degree skirt panel of dryer 2

Attachment D: Acquisition Front-end channel assignment



GENE-0000-0041-1656-01, Revision 2
Non-proprietary Version

A/D CHANNEL ASSIGNMENT

SET A1 & A2 DRY

A/D CHASSIS: 2 LMS Scadas III frontends in master-slave setup.

A/D CHANNEL	SENSOR ID						
1	21233	33	31425	65	8389	97	21869
2	NA	34	31425	66	16224	98	22143
3	36614	35	31425	67	16224	99	18026
4	36614	36	5604	68	16224	100	11156
5	36614	37	5604	69	17102	101	18381
6	37124	38	5604	70	17102	102	18003
7	37124	39	20246	71	17102	103	18025
8	37124	40	20246	72	14386	104	18027
9	37126	41	20246	73	14386	105	8766
10	37126	42	27796	74	14386	106	8767
11	37126	43	27796	75	6682	107	8768
12	37130	44	27796	76	6682	108	21871
13	37130	45	17333	77	6682	109	21852
14	37130	46	17333	78	11750	110	21855
15	37277	47	17333	79	11750		
16	37277	48	5688	80	11750		
17	37277	49	5688	81	16955		
18	37132	50	5688	82	16955		
19	37132	51	5683	83	16955		
20	37132	52	5683	84	15314		
21	37279	53	5683	85	15314		
22	37279	54	31426	86	15314		
23	37279	55	31426	87	16954		
24	37281	56	31426	88	16954		
25	37281	57	15625	89	16954		
26	37281	58	15625	90	220		
27	31423	59	15625	91	264		
28	31423	60	4701	92	8751		
29	31423	61	4701	93	8778		
30	15590	62	4701	94	21857		
31	15590	63	8389	95	21836		
32	15590	64	8389	96	21860		

Data Collected By: _____ **Signature:** _____

Verified By: _____ **Signature:** _____

Date Performed: _____

Test Equip., Serial No. & Calibration Due Date: _____

LMS Scadas III frontend (master)	41011904	09-Mar-06
LMS Scadas III frontend (slave)	41001503	15-Feb-06



GENE-0000-0041-1656-01, Revision 2
Non-proprietary Version

A/D CHANNEL ASSIGNMENT

SET A1&A2 LWL

A/D CHASSIS: 2 LMS Scadas III frontends in master-slave setup

A/D CHANNEL	SENSOR ID						
1	21233	33	31425	65	8389	97	21870
2	NA	34	31425	66	16224	98	22143
3	36614	35	31425	67	16224	99	18026
4	36614	36	5604	68	16224	100	11156
5	36614	37	5604	69	17102	101	18381
6	37124	38	5604	70	17102	102	18003
7	37124	39	20246	71	17102	103	18025
8	37124	40	20246	72	14386	104	18027
9	37126	41	20246	73	14386	105	8766
10	37126	42	27796	74	14386	106	8767
11	37126	43	27796	75	6882	107	8768
12	37130	44	27796	76	6882	108	21871
13	37130	45	17333	77	6882	109	21852
14	37130	46	17333	78	11750	110	21855
15	37277	47	17333	79	11750		
16	37277	48	5688	80	11750		
17	37277	49	5688	81	16955		
18	37132	50	5688	82	16955		
19	37132	51	5683	83	16955		
20	37132	52	5683	84	15314		
21	37279	53	5683	85	15314		
22	37279	54	31426	86	15314		
23	37279	55	31426	87	16954		
24	37281	56	31426	88	16954		
25	37281	57	15625	89	16954		
26	37281	58	15625	90	220		
27	31423	59	15625	91	264		
28	31423	60	4701	92	8751		
29	31423	61	4701	93	8778		
30	15590	62	4701	94	21857		
31	15590	63	8389	95	21836		
32	15590	64	8389	96	21860		

Data Collected By: _____ **Signature:** _____

Verified By: _____ **Signature:** _____

Date Performed: _____

Test Equip., Serial No. & Calibration Due Date: _____

LMS Scadas III frontend (master)	41011904	09-Mar-06
LMS Scadas III frontend (slave)	41001503	15-Feb-06

GENE-0000-0041-1656-01, Revision 2
Non-proprietary Version

A/D CHANNEL ASSIGNMENT

SET B LWL & DRY

SET D LWL & DRY

A/D CHASSIS: 2 LMS Scadas III frontends in master-slave setup

A/D CHANNEL	SENSOR ID						
1	21233	33	21468	65	20248	97	21870
2	NA	34	21468	66	17051	98	22143
3	36616	35	21468	67	17051	99	18026
4	36616	36	6686	68	17051	100	11156
5	36616	37	6686	69	20250	101	18381
6	37125	38	6686	70	20250	102	18003
7	37125	39	8388	71	20250	103	18025
8	37125	40	8388	72	15287	104	18027
9	37129	41	8388	73	15287	105	8766
10	37129	42	28390	74	15287	106	8767
11	37129	43	28390	75	6683	107	8768
12	37131	44	28390	76	6683	108	21871
13	37131	45	15591	77	6683	109	21852
14	37131	46	15591	78	6685	110	21855
15	37278	47	15591	79	6685		
16	37278	48	4702	80	6685		
17	37278	49	4702	81	17106		
18	37275	50	4702	82	17106		
19	37275	51	5683	83	17106		
20	37275	52	5683	84	31042		
21	37280	53	5683	85	31042		
22	37280	54	31426	86	31042		
23	37280	55	31426	87	15333		
24	37282	56	31426	88	15333		
25	37282	57	15625	89	15333		
26	37282	58	15625	90	220		
27	28384	59	15625	91	264		
28	28384	60	4701	92	8751		
29	28384	61	4701	93	8778		
30	27802	62	4701	94	21857		
31	27802	63	20248	95	21836		
32	27802	64	20248	96	21860		

Data Collected By: _____ **Signature:** _____

Verified By: _____ **Signature:** _____

Date Performed: _____

Test Equip., Serial No. & Calibration Due Date: _____

LMS Scadas III frontend (master)	41011904	09-Mar-06
LMS Scadas III frontend (slave)	41001503	15-Feb-06

GENE-0000-0041-1656-01, Revision 2
Non-proprietary Version

A/D CHANNEL ASSIGNMENT

SET C DRY & LWL

A/D CHASSIS: 2 LMS Scadas III frontends in master-slave setup

A/D CHANNEL	SENSOR ID						
1	21233	33	31425	65	8389	97	21870
2	NA	34	31425	66	16224	98	22143
3	36614	35	31425	67	16224	99	18026
4	36614	36	5604	68	16224	100	11156
5	36614	37	5604	69	17102	101	18381
6	37124	38	5604	70	17102	102	18003
7	37124	39	20246	71	17102	103	18025
8	37124	40	20246	72	14386	104	18027
9	37126	41	20246	73	14386	105	8766
10	37126	42	27796	74	14386	106	8767
11	37126	43	27796	75	6682	107	8768
12	37130	44	27796	76	6682	108	21871
13	37130	45	17333	77	6682	109	21852
14	37130	46	17333	78	11750	110	21855
15	37277	47	17333	79	11750		
16	37277	48	5688	80	11750		
17	37277	49	5688	81	16955		
18	37132	50	5688	82	16955		
19	37132	51	5683	83	16955		
20	37132	52	5683	84	15314		
21	37279	53	5683	85	15314		
22	37279	54	31426	86	15314		
23	37279	55	31426	87	16954		
24	37281	56	31426	88	16954		
25	37281	57	15625	89	16954		
26	37281	58	15625	90	220		
27	31423	59	15625	91	264		
28	31423	60	4701	92	8751		
29	31423	61	4701	93	8778		
30	15590	62	4701	94	21857		
31	15590	63	8389	95	21836		
32	15590	64	8389	96	21860		

Data Collected By: _____ **Signature:** _____

Verified By: _____ **Signature:** _____

Date Performed: _____

Test Equip., Serial No. & Calibration Due Date: _____

LMS Scadas III frontend (master)	41011904	09-Mar-06
LMS Scadas III frontend (slave)	41001503	15-Feb-06

GENE-0000-0041-1656-01, Revision 2
Non-proprietary Version

A/D CHANNEL ASSIGNMENT

SET E LWL & DRY

A/D CHASSIS: 2 LMS Scadas III frontends in master-slave setup

A/D CHANNEL	SENSOR ID						
1	21233	33	31425	65	8389	97	21870
2	NA	34	31425	66	16224	98	22143
3	37278	35	31425	67	16224	99	18026
4	37278	36	5604	68	16224	100	11156
5	37278	37	5604	69	17102	101	18381
6	37124	38	5604	70	17102	102	18003
7	37124	39	20246	71	17102	103	18025
8	37124	40	20246	72	14386	104	18027
9	37126	41	20246	73	14386	105	8766
10	37126	42	27796	74	14386	106	8767
11	37126	43	27796	75	6682	107	8768
12	37130	44	27796	76	6682	108	21871
13	37130	45	17333	77	6682	109	21852
14	37130	46	17333	78	11750	110	21855
15	37277	47	17333	79	11750		
16	37277	48	5688	80	11750		
17	37277	49	5688	81	16955		
18	37132	50	5688	82	16955		
19	37132	51	5683	83	16955		
20	37132	52	5683	84	15314		
21	37279	53	5683	85	15314		
22	37279	54	31426	86	15314		
23	37279	55	31426	87	16954		
24	37281	56	31426	88	16954		
25	37281	57	15625	89	16954		
26	37281	58	15625	90	220		
27	31423	59	15625	91	264		
28	31423	60	4701	92	8751		
29	31423	61	4701	93	8778		
30	15590	62	4701	94	21857		
31	15590	63	8389	95	21836		
32	15590	64	8389	96	21860		

Data Collected By: _____ **Signature:** _____

Verified By: _____ **Signature:** _____

Date Performed: _____

Test Equip., Serial No. & Calibration Due Date: _____

LMS Scadas III frontend (master)	41011904	09-Mar-06
LMS Scadas III frontend (slave)	41001503	15-Feb-06

GENE-0000-0041-1656-01, Revision 2
Non-proprietary Version

A/D CHANNEL ASSIGNMENT

Static load test

A/D CHASSIS: 2 LMS Scadas III frontends in master-slave setup

A/D CHANNEL	SENSOR ID						
1	21233	33		65		97	
2		34		66		98	
3		35		67		99	
4		36		68		100	
5		37		69	20250	101	strain
6		38		70	20250	102	strain
7		39		71	20250	103	strain
8		40		72	15287	104	strain
9	37129	41		73	15287	105	strain
10	37129	42		74	15287	106	strain
11	37129	43		75		107	strain
12	37131	44		76		108	strain
13	37131	45		77		109	strain
14	37131	46		78		110	strain
15		47		79		111	strain
16		48		80		112	strain
17		49		81			
18		50		82			
19		51	5683	83			
20		52	5683	84			
21		53	5683	85			
22		54	31426	86			
23		55	31426	87			
24		56	31426	88			
25		57		89			
26		58		90			
27	28384	59		91			
28	28384	60		92			
29	28384	61		93			
30	27802	62		94			
31	27802	63		95			
32	27802	64		96			

Data Collected By: _____ **Signature:** _____

Verified By: _____ **Signature:** _____

Date Performed: _____

Test Equip., Serial No. & Calibration Due Date: _____

LMS Scadas III frontend (master)	41011904	09-Mar-06
LMS Scadas III frontend (slave)	41001503	15-Feb-06

Attachment E: Test Log Sheets

GENE-0000-0041-1656-01, Revision 2
 Non-proprietary Version

①

Data Log

MoRLp-Div-050920-Set A1 Run Name

Title of Test	Impact Hammer Location	Data Filename	Date and Time of Acquisition	Gain Settings
0509-A1	skir-781-X1		050901 10:57	
	skir-781-X2			
	skir-782-X1		11:05	
	skir-783-X1		11:10	
	skir-784-X1		11:14	
	skir-785-X1		11:18	
	skir-786-X1		11:24	
	skir-787-X1		11:28	
	skir-788-X1		11:34	
	skir-789-X1		11:39	
	skir-790-X1		11:44	
	skir-791-X1		11:50	
	skir-792-X1		11:55	
	skir-793-X1		12:01	
	skir-794-X1		12:07	
	skir-795-X1		12:13	
	skir-796-X1		12:19	
	skir-797-X1		12:25	
	skir-798-X1		12:31	
	skir-799-X1		12:37	
	skir-7421-X1		050901 1440	

brown red trip

switch to under accel sensor spring switch to hand sledge red tip

Switch to 1924Hz

Data Collected By: Lesperoy/Falbo Signature: [Signature]
 Verified By: Neiheisel Signature: [Signature]
 Date Performed: 01/14/05
 Test Equip., Serial No. & Calibration Due Date: _____

GENE-0000-0041-1656-01, Revision 2
 Non-proprietary Version

Data Log

Mod Ip LWL 050501a Set A1

Title of Test	Impact Hammer Location	Data Filename	Date and Time of Acquisition	Gain Settings
A1	Skir 781 X		9:30pm 050501	/
	783 X			/
	784 X			/
	785 X			/
	789 X			/
	787 X			/
	hola 187 X		Very low DP response Fixed by adjusting gains up & down	/
	hola 787 X			/
	Skir 788 X		Softer hit to prevent overloads	/
	779 X		X1 bad	X
			x2 soft hits	/
	786 X		Soft. Data checked	/
			785 & 787 low response	/
	778 X		Soft hits	/
	787 X		Soft	/
B1 LWL	hola 782 X		2:50am	
			Some low reals	
	783 X		Very low response 267 X ch # 110	/
	784 X		"	/
	785 X		"	/
	781 X		"	/
	782 X 2		Some low 253 & y 251 & y 252 & y 281 & y 277 & y 262 & y 260 & y	

Data Collected By: Mel. & E. Sundstrom Signature: [Signature]

Verified By: Neiheisel Signature: [Signature]

Date Performed: 050501/050502 Alex S. & A.

Test Equip., Serial No. & Calibration Due Date:

GENE-0000-0041-1656-01, Revision 2
 Non-proprietary Version

5

Data Log

Mod Imp Dry - 050502a - Set B1

Title of Test	Impact Hammer/Location	Data Filename	Date and Time of Acquisition	Gain Settings
Set B1	SK: 781-X1		050502	0502
	hda: 182-X			Incorrect cal
	hdb: 782-X			added Triax 30 at hdb: 779
	hdb: 781-X			
	hdb: 983-X			
	hdb: 884-X			
	Rdb: 785-X			9:32
	Mod Imp Dry	050502a	Set C	
Set C	hdb: 282-X1		050502	1240
	hda: 182-X1			
	Replaced	TRAX 30 with 37, ran TRAX 20		straight to front
	hda: 182-X2			15:20
	hda: 184-X1		050502	1348
	hda: 185-X1		050502	1357
	hda: 183-X1			
	hda: 186-X1			
	shir: 781-X1			
	SK: 782-Y1		050502	1435
Set D	Replaced #70x	accel - but triax cable		
	Ch 8)	(added single to triax)		

See notes
 driving point may be incorrect

front

B1 Lesparoy / Falbo
 Data Collected By: C. Weikheil / Jonckheere Signature: *[Signature]*
 Verified By: Melitz Signature: *[Signature]*
 Date Performed: 050502
 Test Equip., Serial No. & Calibration Due Date:

GENE-0000-0041-1656-01, Revision 2
Non-proprietary Version

⑦

Data Log				
Section: <i>Mod Imp LVL 050502 set D</i>				
Title of Test	Impact Hammer Location	Data Filename	Date and Time of Acquisition	Gain Settings
set D	holb 282 X	0435	Accl removal by accident	
cont			3 retests	
			Bad response on charge,	
			switch to ICP	
	holb 282 X 2		Best side 504 all directions	
	holb 282 X 3		Tighten wire to scall	✓
	ring 482 X 2	1430		✓
	ring 482 X			✓
	side 682 y			✓
	side 681 y			✓
			Water pump start 2400	
			stop 3445	
set D	Dry	48415		
	side 681 y			✓
	side 682 y			✓
	ring 482 X			✓
	ring 483 X			✓
	holb 282 X			✓
	supp 983 y			✓
	supp 982 X			✓
	side 981 X			✓
	side 583 y	5400		✓
	side 582 y		Some low strange rattle/reverb noise - hard to find	✓
	ring 481 y			✓
	holb 182 X			✓
	skir 781 X			✓

Data Collected By: *Melitz/Sandstrom* Signature: *[Signature]*

Verified By: *Neikeisel* Signature: *[Signature]*

Date Performed: *050503* *[Signature]*

Test Equip., Serial No. & Calibration Due Date:



8

Data Log

Mod Imp_Dry^{DRY} - 050503 - Set E

Title of Test	Impact Hammer Location	Data Filename	Date and Time of Acquisition	Gain Settings
Section Set E	top: 884 - Z-A top: 888 - Z-A		10:15 top: 816 → plastic isolation	
		→ after installation of point	top: 816 result is much better.	
	top: 882 - Z1		had driving point (checked)	
	top: 888 - Z1		→ top: 812 had SREF (checked)	
	top: 884 - Z1		→ had DP had SREF top: 812 (checked)	
	top: 885 - Z1		→ good DP → JCP had SREF top: 812	
	WS: 883 - X1		→ good DP (checked) had SREF 812	
	top: 882 - X1 top: 882 - X1		→ had DP (checked) JCP	
	top: 881 - X		→ good DP had SREF = 812	

Data Collected By: Lesperoy/Falbo Signature: [Signature]
 Verified By: Neihasel Signature: [Signature]
 Date Performed: 050503
 Test Equip., Serial No. & Calibration Due Date: _____



(10)

Data Log

TDG + BN 060603
 8.1h10

Title of Test	Impact Hammer Location	Data Filename	Date and Time of Acquisition	Gain Settings
1st	150% 6p 1% 19		rather low for most all	1 hit only
2nd	15 dk			
	↑ Insert bridge ch info		not pushed!	
Time	995 - 7	01 dk	missed	1701 11:00
1st	struck tool	02 dk		1101 11:00
2nd	bridge	03 dk		1101 11:00
	hit	04 dk		1101 11:00
		05 dk		1101 11:00
		06 dk		1101 11:00
		07 dk		1101 11:00
		08 dk		1101 11:00
		09 dk		1101 11:00
		10 dk		1101 11:00
1st	bridge	05	para. to 2	500, 1000, 10000
Fixed	10			
Time	995 2	11	some under loads	
1st		12 dk	better	
		13 dk		
	995 - 7	1	hitting requires to soft hits	
	995 + 8	1 dk		
		2 dk		
		3 dk		
		4 dk		
Time	997 2	1 dk	miss: ok	gap: dir (A)
1st		2 dk	" " "	" "
	Unif. Unif	3 "	" " "	" "
		4 "	" " "	" "
		5 "	" " "	" "
		6 dk	" " "	" "
		7 dk	" " "	" "
		8 dk	" " "	" "
		9 dk	" " "	" "
		10 dk	" " "	" "
Time	999 + X	5 dk		
		6 dk	double hit	

997 2

Data Collected By: Unif
 Verified By: Unif
 Date Performed: 03 Mag 15
 Test Equip., Serial No. & Calibration Due Date:

Signature: [Signature]
 Signature: [Signature]
 Signature: [Signature]

Melitz / De Bta Brabandere
 Nekeisel

[Signature]
 Michael Thibault

GENE-0000-0041-1656-01, Revision 2
 Non-proprietary Version

(11)

Data Log

23h30
 ↑

Title of Test	Impact Hammer Location	Data Filename	Date and Time of Acquisition	Gain Settings
781 GVS	779 JV 19	Unif Unit	Accept: OK	YASAC: noise 0m
	5mms 4m 10	FE% tip 12		
	inusable			
782 GVS	787 JX 10 OK			
	PANEL 90°			
783 GVS	783 -X 1 ok	FE% tip 12	5mms 1 bed sq channel	795 A ch
	784 -X 1 ok			
	785 -X 1 ok			
	785 -X time	Unif Unit	1 ok	
		3		
	786 -X time	1		
		2		
		3		
	783 -X time	1		
		2		
		3		
		4		
		5		
		2		
		9,10	No double hit	only steel
	784 -X Time	5, 6, 7, 8	No double hit	
	785 -X Time	4, 5, 6		
	789 -X Time	1, 2, 3		
	781 -X Time	1, 2, 3		

106
 ff

Hook time - small
 double hit ok

Data Collected By: Melite/Sandstrom Signature: *[Signature]*
 Verified By: Neheisel Signature: *[Signature]*
 Date Performed: 03 May 05 / 04 May 05 → *[Signature]*
 Test Equip., Serial No. & Calibration Due Date:

GENE-0000-0041-1656-01, Revision 2
 Non-proprietary Version

12

Data Log

5/4/05

Title of Test	Inspect Hammer Location	Data Filename	Date and Time of Acquisition	Gain Settings
	SEF 721 - x Log	01670	OK	
	hda 185 x	ok	Strain 197A dead	
	hda 185 x Time	ok	Low	
		ok 2	Noisy	
	hda 186 Time 1	ok		
	186 = 112			
		ok		
	hda 186 Log 1	ok	Strain EPLS noisy	
	hda 197			
	197 = 192			
	Static Load	Very Slow	2 or 3 channels	5
	2	Fast		280
	3	fast		30-40
	4	"		
	5	"		
			050504	0.00

Data Collected By: Melitz/Sandstrom Signature: *[Signature]*

Verified By: Heikesel Signature: *[Signature]*

Date Performed: 04 May 05 *[Signature]*

Test Equip., Serial No. & Calibration Due Date: